

AUTOMATED PHASE DENSITIES AND INTERFACIAL
TENSION MEASUREMENTS

By

KURTIS VAUGHN ROUSH

Bachelor of Science

Oklahoma State University

Stillwater, Oklahoma

1989

Submitted to the Faculty of the
Graduate College of the
Oklahoma State University
in partial fulfillment of
the requirements for
the Degree of
MASTER OF SCIENCE
July, 1991

Thesis
1991
R863a
cop. 2

AUTOMATED PHASE DENSITIES AND INTERFACIAL
TENSION MEASUREMENTS

Thesis Approved:

K.A.M. GASSM

Thesis Adviser

Ailand H. Johannes

Luth C. Galar

Norman N. Dusho

Dean of the Graduate College

PREFACE

A vapor-liquid equilibrium experimental facility designed for the measurement of phase densities and interfacial tensions (IFT) at various temperatures was automated. The automation provides for computerized data acquisition and temperature control as well as instantaneous analysis of the raw data. In addition, a new IFT cell was designed and constructed, and a number of components of the apparatus which have hindered progress in previous endeavors were modified.

The automation of the experimental apparatus was successful in both controlling the system temperature within 0.1°F and acquiring vapor pressure, liquid and vapor densities, and interfacial tension of pure fluids. Precise vapor pressure, phase densities, and interfacial tension data were obtained for n-pentane at 120°F. Comparison of the results of this test case with reliable literature measurements confirm the viability of the automated apparatus.

I would like to thank Dr. R. L. Robinson, Jr., Dr. Ruth Erbar, Dr. M. Stone, my advisor K. A. M. Gasem whose friendship and support helped me to reach my potential, and Dr. A. H. Johannes, "A.J.", who showed me a glimpse of the capabilities of a microcomputer.

I want to express my deepest gratitude to my wife Lori, whose enduring patience allowed me to give my full attention to this endeavor. Finally, this humble effort is dedicated to my beloved father who taught me God's principle of working diligently.

TABLE OF CONTENTS

| Chapter | Page |
|--|------|
| I. INTRODUCTION | 1 |
| II. LITERATURE REVIEW. | 4 |
| Methods for Determining Interfacial Tension (IFT) | 4 |
| IFT Measured from Discrete Points. | 5 |
| IFT Measured from Data Encompassing the Drop Profile. | 7 |
| Automated Systems | 9 |
| III. APPARATUS MODIFICATIONS. | 13 |
| Air Bath. | 16 |
| IFT Cell. | 17 |
| Liquid Density Meter. | 22 |
| Fluid Injection Pump. | 22 |
| IV. AUTOMATION | 24 |
| Acquisition and Control | 25 |
| Computer | 28 |
| External Input/Output Modules. | 28 |
| Controllers. | 30 |
| Microsoft OS/2 | 31 |
| Labtech Control. | 31 |
| Grapher. | 32 |
| IFT Determination | 32 |
| Computer | 33 |
| Video Equipment. | 33 |
| Imaging Software | 33 |
| IFT Routines | 34 |
| Integration of Automation Equipment | 34 |
| V. EXPERIMENTAL PROCEDURE | 38 |
| Apparatus Clean-up. | 39 |
| System Calibration. | 40 |
| Pressure Testing. | 43 |
| Data Acquisition. | 43 |
| VI. EXPERIMENTAL RESULTS AND DISCUSSION. | 47 |
| Experimental Data | 47 |

| Chapter | Page |
|---|------|
| Discussion. | 54 |
| VII. CONCLUSIONS AND RECOMMENDATIONS. | 58 |
| Conclusions | 58 |
| Recommendations | 59 |
| LITERATURE CITED. | 61 |
| APPENDIXES. | 64 |
| APPENDIX A - SYSTEM INTEGRATION. | 64 |
| APPENDIX B - STEP TESTS. | 87 |
| APPENDIX C - CALIBRATIONS. | 96 |
| APPENDIX D - ERROR ANALYSIS. | 107 |

LIST OF TABLES

| Table | Page |
|--|------|
| I. Comparison of Experimental and Literature Values for Vapor Pressure and Density of n-C ₅ at 120°F. | 48 |
| II. Comparison of Experimental and Literature Values for $\gamma/\Delta\rho$ for n-C ₅ at 120°F. | 49 |

LIST OF FIGURES

| Figure | Page |
|--|------|
| 1. Drop Profile Analyzed by the Discrete Method | 6 |
| 2. Complete Drop Profile Analysis | 6 |
| 3. Experimental Facility Showing the Vapor Flow Path. | 14 |
| 4. Experimental Facility Showing the Liquid Flow Path | 15 |
| 5. Simplified Diagram of the Existing IFT Cell. | 18 |
| 6. Schematic of the IFT Cell Prototype. | 21 |
| 7. Automated System Overview. | 26 |
| 8. Automated Acquisition and Control Scheme | 27 |
| 9. IFT Valve Configuration. | 46 |
| 10. Typical Edge Traced Drop Profile | 52 |
| 11. Typical Translated and Converted Drop Profile. | 53 |
| 12. Integrated Profile Residual for the 0.0355 Inch Needle | 55 |

CHAPTER I

INTRODUCTION

Design and operation of separation equipment requires knowledge of fluid phase behavior. Development of models for the accurate description of the phase behavior of a variety of chemical species, in turn, places heavy demands for reliable vapor-liquid equilibrium (VLE) data. While compositions and densities of co-existing phases constitute the basic VLE thermodynamic properties in most applications, accurate interfacial tensions (IFT) are the essential complement in describing numerous phenomena of interest. Enhanced oil recovery operations, design of extraction equipment exemplify the need for IFT data in the energy sector. Additionally, the studies of vapor-liquid interfaces find many applications from the food and cosmetic industry to the study of interfacial interaction in biological cell membranes. However, one of the main drawbacks in the study of thermodynamic interfacial properties has been the difficulty associated with the measurement of interfacial tension, especially in high pressure - high temperature environments (1).

An experimental facility has been established and operated at Oklahoma State University for the measurement of a number of thermodynamic equilibrium properties at elevated temperatures and pressures. These properties include liquid and vapor density, interfacial tension, and phase compositions. During the first phase of

operation, the facility was utilized to obtain valuable equilibrium measurements on binary and multicomponent CO₂/ethane-hydrocarbon systems which were of interest to the energy sector (2-4).

During the previous research, most of the data acquisition and control was handled manually. The system temperature control was fine tuned manually through the use of multiple cartridge heaters powered by voltage transformers. Liquid and vapor densities, temperature, and pressure were recorded by hand from the corresponding instrument readout and the interfacial tensions were determined by the manual analysis of enlarged photographic negatives of pendant drops. Therefore, the data acquisition and control tasks of the previous research endeavors were time consuming, especially in dealing with temperature control and the analysis of pendant drops for the determination of IFT's.

The goal of this work was two fold: first, computer automation of the existing experimental facility, and second, establishing the reliability of the automated system by comparing newly acquired data with the corresponding literature values. Automated data acquisition and control was accomplished by interfacing a microcomputer with a stand alone external input/output (I/O) device via RS-232. Temperature control was affected by the integration of circuit controllers designed for temperature control to within 0.1°F. In addition, the existing method of determining interfacial tensions was replaced with a more efficient and accurate method. Namely, the incorporation of a video image processor to digitize the pendant drop profile and determine interfacial tension based on the complete profile analysis. A test run involving the measurement of vapor pressure, phase densities, and

interfacial tension of a selected pure hydrocarbon, namely n-C₅, was performed. A careful comparison with literature values was undertaken to validate the effectiveness of the new system.

The work presented here is limited to the automation of the existing facility for the study of pure fluid properties. Although the integration of the existing gas chromatograph for multicomponent studies is possible using the new automated system, the task is beyond the scope of this work.

CHAPTER II

LITERATURE REVIEW

During the course of this study, a survey of relevant literature was conducted. The survey was limited to two topics: 1) the study of interfacial tensions, and in particular, the measurement and determination of interfacial tensions using the pendant drop method, and 2) the automation of vapor-liquid equilibrium systems. Although many of the studies reviewed apply different techniques for determining interfacial tension, the attention in this study was directed toward the pendant drop method.

Methods for Determining Interfacial Tension

Determination of the interfacial tension (IFT) from a pendant or sessile drop has been around for a long time. The mathematical treatment based on the Laplace equation (5) for curved surfaces was developed by Bashforth and Adams (6) around 1883 and used by Andreas, Hauser, and Tucker (7) to measure the boundary tension of a pendant drop in 1938 (8). Until recently, the determination of the IFT from pendant drops was primarily achieved by measuring the characteristic diameters of the drop profile from a photographic negative or plate as with Andreas, Hauser, and Tucker. These diameters were then used to calculate a shape parameter and correlated to solutions of the fundamental differential equation. With the advances in microcomputer

and video image technology, more recent studies evaluate IFT by numerically integrating the Young-Laplace equation and utilizing the data encompassing the entire drop profile (9-12).

IFT Measured from Discrete Points

Andreas, Hauser, and Tucker (7) describe a technique which involves the measurement of D_e , the maximum diameter, and D_s , the diameter of the drop measured a distance D_e from the apex (see Figure 1). The shape of the drop is then characterized by the parameter S , where

$$S = D_s/D_e \quad (1)$$

The IFT may then be calculated by:

$$\gamma = g\Delta\rho D_e^2/H \quad (2)$$

where

γ is the interfacial tension

g is the local gravity

$\Delta\rho$ is the difference in liquid and vapor density

H is a correction factor

The factor H is dependent upon the shape of the drop profile. Andreas, et al. provided a table of $1/H$ as a function of S which was obtained experimentally. Later refinements of $1/H$ as a function of S were added with the numerical solution of the differential equation described by Bashforth and Adams (13,14). Dulcamara (15) implemented a method of least squares on tabulated data by Mills (16) and arrived at the equation:

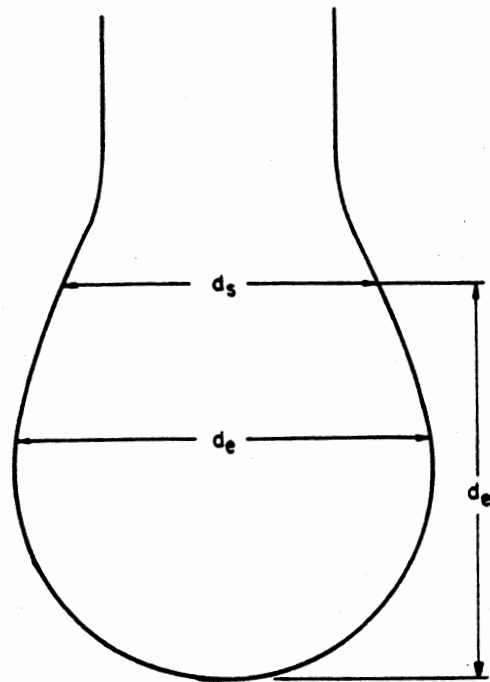


Figure 1. Drop Profile Analyzed by the Discrete Point Technique

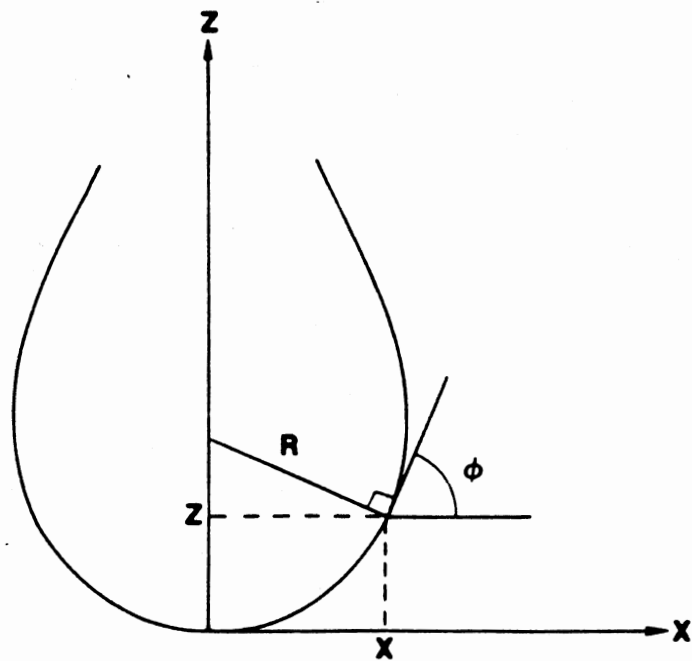


Figure 2. Complete Drop Profile Analysis

$$1/H = 0.31470 S^{-2.62529} \quad (3)$$

The parameter S is not unique in that any other characteristic diameter ratio may be used. Other studies have been done utilizing multiple diameters (17) or minimum diameters (18).

The errors associated with a characteristic diameters method as described by Andreas, et al. were analyzed by Stauffer (19). He surmised that the error in the method was 2 to 6% for the usual size of drops encountered in practice for a 1% error in the measurement of the drop dimensions. Abwani and Fort (20) estimated an error of $\pm 0.15\%$ if the dimensions of the selected plane had an accuracy of $\pm 0.06\%$ (8).

IFT Measured from Data Encompassing the Drop Profile

Despite the simplicity of calculating IFT's with the discrete point method of Andreas, et al. the level of uncertainty in the resultant measurements precludes high precision. Most pendant drop procedures utilize characteristic diameters of the drop profile to describe the whole drop surface. These discrete points are critical since they correspond to special features, such as inflection points on the interface, and they must be calculated with a high degree of accuracy (21). Therefore, coinciding with advances in computing and image processing, a different IFT calculation procedure has emerged. Mainly, the utilization of data points encompassing the whole drop profile for the numerical integration of the Young-Laplace equation describing the profile.

As detailed by Rotenberg, et al. (21) the Young-Laplace equation may be described as a set of three first-order differential equations:

$$dx/ds = \cos \phi \quad (4)$$

$$dz/ds = \sin \phi \quad (5)$$

$$d\phi/ds = 2 + \beta z - \sin \phi/x \quad (6)$$

its derivatives with respect to β are:

$$dx'/ds = -\phi' \sin \phi \quad (7)$$

$$dz'/ds = \phi' \cos \phi \quad (8)$$

$$d\phi'/ds = z + \beta z' - \frac{\phi' \cos \phi}{x} + \frac{x' \sin \phi}{x^2} \quad (9)$$

$$\beta = \Delta \rho g (R_0^2) / \gamma \quad (10)$$

where,

x, z are the drop profile coordinates reduced by R_0

R_0 is the radius of curvature at the apex

s is the reduced arc length from the apex to the point

ϕ is the turning angle at the point

(see figure 2).

Rotenberg, et al., solved these equations using a Newton-Raphson technique and later refined the routine by combining it with the method of incremental loading. Other Authors have used similar techniques for the calculation of IFT (9-12).

Jennings and Pallas (22) concluded that using the Rotenberg procedure resulted in the inefficient use of cpu time. As an example they cite that the time required to analyze 500 profiles each of 1000 coordinates using the technique of Rotenberg took 64 hours of cpu time on a VAX 8600. Jennings and Pallas present an optimization technique

based on the rotational discrimination method which they report as being "superior to the previously used Newton-Raphson technique (21) in several aspects". The cpu time required to fully analyze the data is reduced 4-50 times with no loss in precision or accuracy. The time reduction is based on the fact that rotational discrimination requires fewer evaluations of the objective function than the Newton-Raphson method and does not require second derivative evaluations. For a detailed description of the rotational discrimination technique see the works of Pallas and Law (22,23).

For use in this work, the method of rotational discrimination by Jennings and Pallas was employed for the IFT determination. A Fortran Program provided by the authors for use on a VAX system was adapted for use on a PC in this study. Previous work using this experimental apparatus has relied on the discrete point method for determining the IFT. A comparison of these two methods is presented in a later chapter.

Automated Systems

The first reported use of automatic control is attributed to the use of a flyball governor on Watts's steam engine around 1775, and the first mathematical analysis of automatic control came from James C. Maxwell in 1868 as he discussed the governor (24). The application of process control in industry, however, did not start until the 1930's, and by the 1940's rather complex control networks were in common use. Today, with advances in digital and analog processing, the field of automation has found new applications in numerous environments where precise acquisition and control are desired.

In this study, the experimental apparatus is capable of controlling the system temperature to within 0.1°F while simultaneously acquiring the VLE pressure, liquid and vapor density, and image profiles, which are later analyzed to determine the interfacial tension. A survey of the automated equipment used in this study follows.

As stated above, the acquisition and control of temperature and pressure is not new. However, the acquisition and control of these variables with a microcomputer is only as new as the microcomputers themselves. There is much literature on the acquisition and control of temperature and pressure. In fact any control textbook will provide the relevant theory as well as descriptions of numerous applications. Due to the long time availability of acquisition and control of temperature and pressure and its wide spread application, a detailed discussion is not presented here.

A few types of in-situ density meters have been employed in recent research, the most common being the vibrating U-tube. The U-tube density meter measurements rely on the ability to correlate the resonant frequency of known fluids with their densities and interpolate the density of a sample from its unique frequency. These density meters are amenable to automatic acquisition and have been used with BCD and RS-232 output formats since the late 1970's (see, e.g., 2-4). Recently, Vernov, et al. (25) have developed a microprocessor-based control unit for the vibrating U-tube. They reported that the addition of a microprocessor-based data-processing and control unit made it possible to increase the accuracy of vibrating measuring instruments by enabling statistical processing of the results, allowing for the main

destabilizing factors to be accounted for and the results to be suitably corrected.

Another type of in-situ density meter beginning to gain recognition is the magnetic density meter. Developed by Okada et al. (26,27) it employs a magnetic buoy, a sample cell, an electromagnetic coil, and a positioner. The underlying principle is that the buoy, immersed in a fluid, is elevated by a magnetic force generated by the coil. In practice, detachment of the buoy from the positioner determines the balancing point of the electromagnetic force and the buoyancy. The DC current and the buoy physical properties can then be related to determine the sample fluid density.

The automated acquisition of interfacial tension has been accomplished in a number of ways. A most common approach employs a needle on which the drop is suspended and a syringe to displace the fluid (12,28). The automation of such a device deals only with the capturing of images and the consequent image analysis. The ability to form a pendant drop is still a trial-and-error procedure. Once the drop is pendant, the image is captured either on film or by image digitization. The latter development has led to techniques in acquiring the drop profile coordinates.

Commercial vendors provide the needed software programs to supplement the digitizing cards used to extract the profile coordinates. The most common being a trace of the edge coordinates around the profile. Use of such techniques for the study of interfacial tension was proposed by Girault, Schiffrin, and Smith (1) in 1982. After experimenting with their system, Girault, et al. concluded that the edge tracing technique had two problems: 1) since

the only information required to measure the boundary tension is the coordinates of a well defined shape, most of the information generated by edge tracing techniques is redundant and complicates further analysis and 2), the edge tracing technique is slow since it analyzes every possible coordinate. They then decided to produce a video image profile digitizer (8) that in essence scans across the image at intervals instead of edge tracing the whole profile. This results in a faster analysis of the profile and less redundant data for IFT determination. Although the method is more efficient than employing the edge tracing technique, no comparable improvement in the accuracy is produced.

There seems to be very little literature dealing with an automated system comparable to the one in this study. Many of the articles published deal with determining interfacial tension by using a syringe for fluid displacements which limits the range of pressures studied. Anastasiadis and co-workers (29) operated an experimental apparatus utilizing temperature control to within 1°C, in-situ U-tube density meters, a video camera, and image digitizing board to study the interfacial tension of immiscible blends. Their experimental apparatus is comparable to the one used in this study, barring the lower precision of the temperature control and the use of a syringe for pendant drop formation. Whether or not the facility of Anastasiadis et al. utilizes a computer for temperature control and data acquisition for instantaneous conversion of raw data is unknown.

CHAPTER III

APPARATUS MODIFICATIONS

The existing experimental apparatus has been well documented in the past, however the most current description is well presented by Dulcamara (15). Briefly, the apparatus consists of five main components: 1) PVT cell, 2) vapor density meter (VDMA) cell, 3) liquid density meter (LDMA) cell, 4) interfacial tension (IFT) cell, and 5) magnetic pump, all which are housed in a constant temperature oven. The system has the ability to circulate fluids in the vapor or liquid phase (see Figures 3 and 4). Vapor circulation insures that only vapor will be present in the VDMA, while liquid circulation insures that only liquid is present in the LDMA cell and that liquid is passed through the top of the IFT cell.

Under previous support from industrial sponsors, the experimental facility produced valuable data on equilibrium phase compositions, densities, and interfacial tensions (2-4). Precise data have been obtained on both pure fluids and mixtures at temperatures extending from 100°F to 268°F and pressures to 5000 psia. Such measurements are designed to elucidate the effects of temperature, pressure, and composition on phase densities and interfacial tensions.

Experience with the apparatus has led to the enhancement of certain components which have hindered the progress in past research endeavors. These enhancements include modifications to the heating

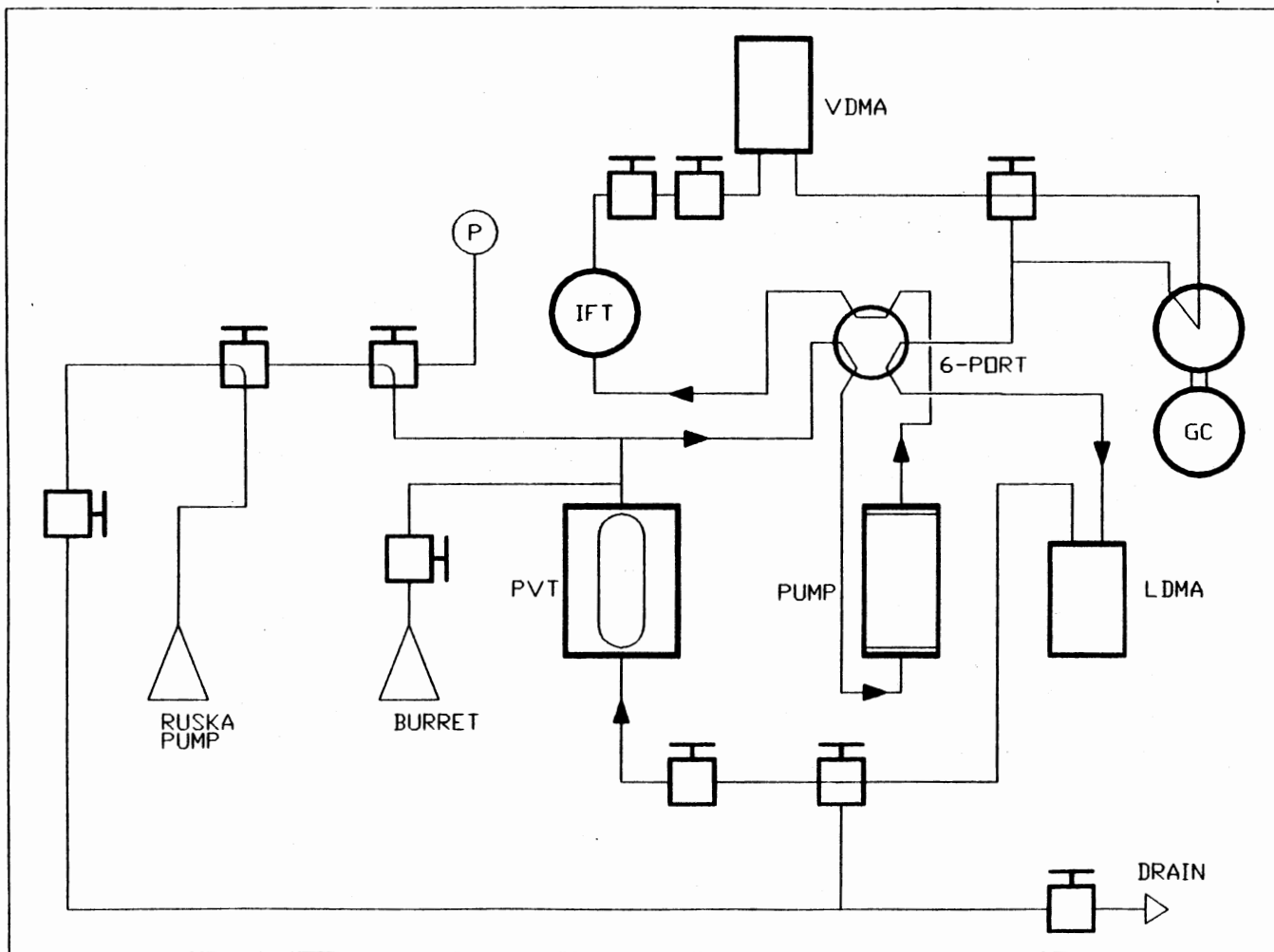


Figure 3. Experimental Facility Showing the Vapor Flow Path

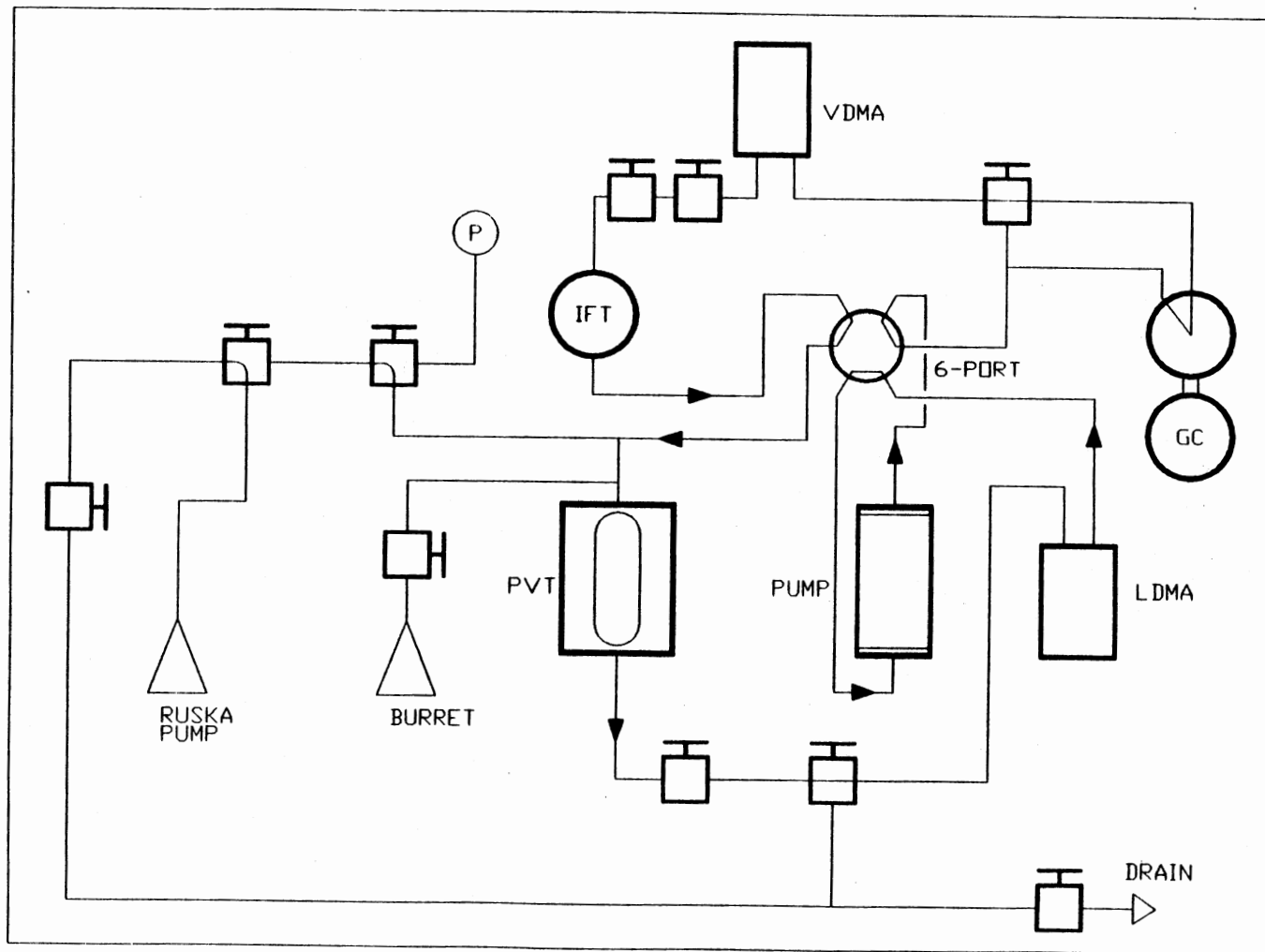


Figure 4. Experimental Facility Showing the Liquid Flow Path

system, IFT cell, LDMA cell, and gas injection pump.

Air Bath

The experimental apparatus is housed within a Hot Pack oven (model 212052-29) which utilizes a 5 kilowatt heater for on/off control. The small heat leaks from the oven combined with the poor control characteristics of the on/off controller have typically produced an oven temperature control within 0.3°F . Moreover, due to the imprecision of the controller set point dial, a trial-and-error procedure is required to attain the desired temperature set point.

To affect temperature control within 0.1°F , in the past, an auxiliary PID controller (Hallikainen, Thermotrol, model 1053) for fine tuning temperature control was employed. That is, once a rough approximation of the desired temperature was obtained from the 5 kilowatt on/off unit, the PID controller with a 500 watt tape heater was then used. In addition, once the desired set point was reached, efforts were directed at eliminating temperature variations (or profiles) within the oven by using separate local heaters. These heaters (150 watt cartridge heaters) are powered by individual Variac autotransformers, which allow for precise manual adjustment of the heat output.

In this work, the time consuming trial-and-error approach to temperature control was replaced with a very efficient system. The original Hot Pack controller was replaced with a Watlow 900 series PID controller. The controller readout allows the selection of a temperature to within 0.1°F . Using this unit, a temperature control within 0.2°F is reached in less than two hours, a marked improvement

over the original controller. The Thermotrol controller used with the tape heater and the manual autotransformers used with the cartridge heaters were replaced with specially designed controllers that utilize a 0-10 volt input monitored by computer software designed to maintain temperatures throughout the oven to within 0.1°F. The computer, software, and controllers used in the air bath are discussed in more detail in chapter IV.

IFT Cell

The IFT cell, manufactured by Temco, was used in previous studies to measure fluid interfacial tensions (see Figure 5). The cell consists of a pressure vessel with observation ports on both ends. Within the cell cavity is a turret which may be rotated by the operator during data acquisition. The turret may contain up to five needles or wires which project in a pentagonal manner in a common plane toward the center of the cell. During normal operation, the turret is rotated by two external handles to vertically align the desired needle with the inlet port (15). Liquid is then squeezed through the needle until a pendant drop forms at the end. The pendant drops suspended from the turret needles are backlit by an optic fiber point source and viewed through a microscope. Photographs are taken of the pendant drops and later analyzed to determine the interfacial tension of the fluid under study.

The viewing port covers, the external handles, and turret inlet port use O-rings. A number of difficulties have been encountered which are attributed to reliance on these O-rings, including:

- 1) leaks at elevated pressures. While reasonable performance was

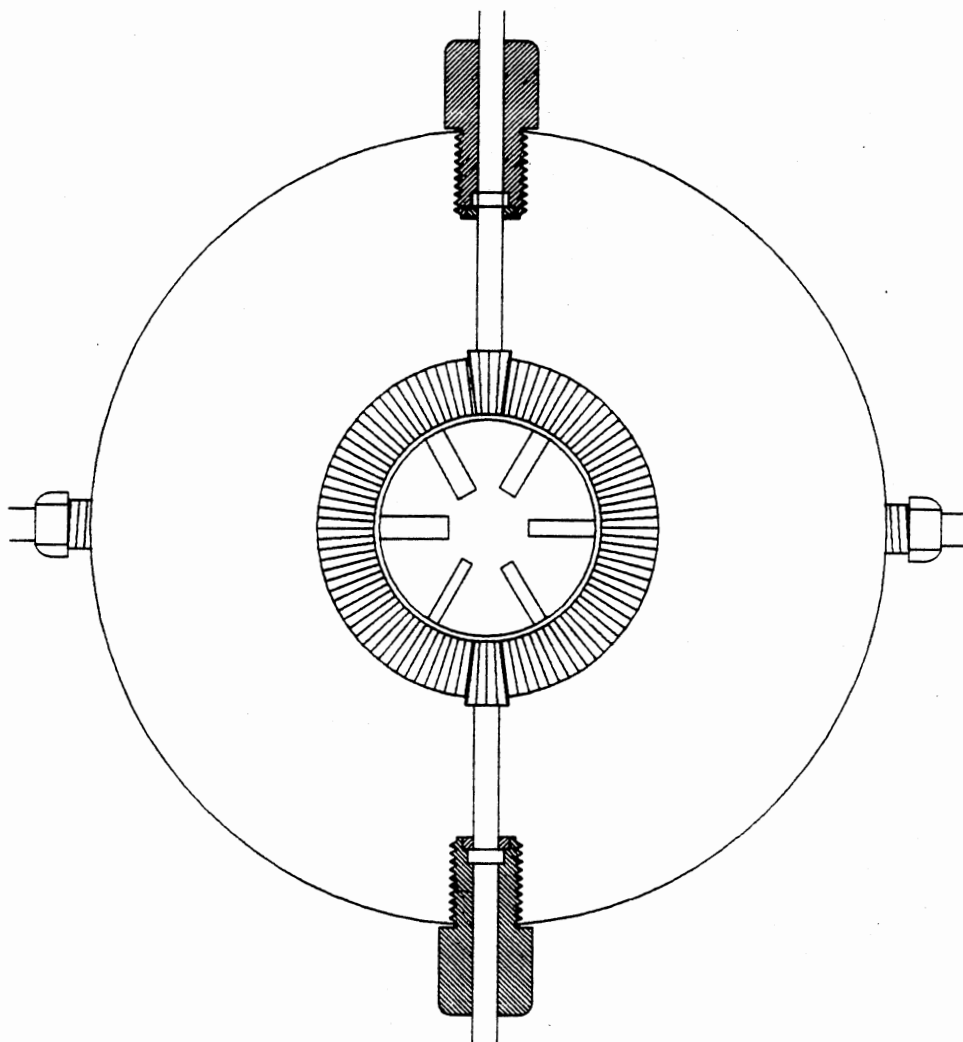


Figure 5. Simplified Diagram of the Existing IFT Cell

obtained from the IFT cell for pressures within 3000 psi, major difficulties were experienced at higher pressures. Attempts to prevent the leaks by tightening the IFT handles were mostly ineffective and hindered the ability to rotate the turret.

- 2) excessive demand for maintenance. Following each experiment, all O-rings require replacement. Damage caused by "explosive decompression" renders the O-rings for the IFT covers useless.
- 3) O-ring swelling. Variations in the chemical nature of the fluids under study lead to differing degrees of swelling in the turret viton O-rings. To prevent O-ring shearing and the resulting formation of residues within the IFT cell, a trial-and-error procedure is typically undertaken to adjust the rise in the turret O-rings.

Attempts to modify the IFT cell such as using different O-rings, reconfiguring the handle design with additional gears outside the cell to alleviate the operator torque required to rotate the turret, and redesigning the turret gear system have all failed. This led to the development of a totally new design.

The new IFT cell design is very simple conceptually and mechanically. The design is basically a rectangular visual high pressure cell. On the broad top side of the cell, four holes are drilled to house needles of various sizes. A hole is drilled into the bottom and serves as an outlet port. Each of the needles have a separate shut-off valve directly upstream which allows for individual needles to be utilized at any time.

To explore the merits of this new design, a discarded high

pressure Wagoner flow meter was employed in constructing the prototype for the IFT cell. Specifically, the flow meter is positioned horizontally with four 5/8" NPT holes bored into the top as inlet ports and one into the bottom as an outlet port (see Figure 6). The threaded holes are then fit with a 5/8" male NPT to 1/4" male Swagelock fitting. Four 2" needles with varied diameters are inserted into individual teflon plugs and then inserted into 1/4" tubing fit with a female Swagelock fitting. The teflon plugs are sized to fit into the 1/4" tubing and are approximately 1/8" long. The four needles are then inserted into the top NPT fittings and the Swagelock fittings are tightened. Each needle line utilizes a valve upstream for selection of an individual needle. The bottom port consists of the same 5/8" NPT-Swagelock fitting and is used to join the IFT cell to the rest of the system via the Swagelock fitting.

The two main advantages of this design are (1) the IFT cell does not have any moving parts, and (2) no O-rings are employed. Actually, the only seals present in this cell involve the high pressure cell gaskets and the swagelock fittings, which are known to produce leak-free seals. The only disadvantage in the current design is that the 2" needles may be off vertically by a few degrees. When such deviations in the needle positioning do occur, the entire IFT cell mounting may be offset to achieve a vertical position.

In addition to replacing the IFT cell, the backlighting unit was modified. The previous IFT cell utilized an optic fiber point source which was located just behind the tip of the vertical needle. Since the turret rotated, no positioning of the light source was necessary when additional needles were used. With the new cell, however, the

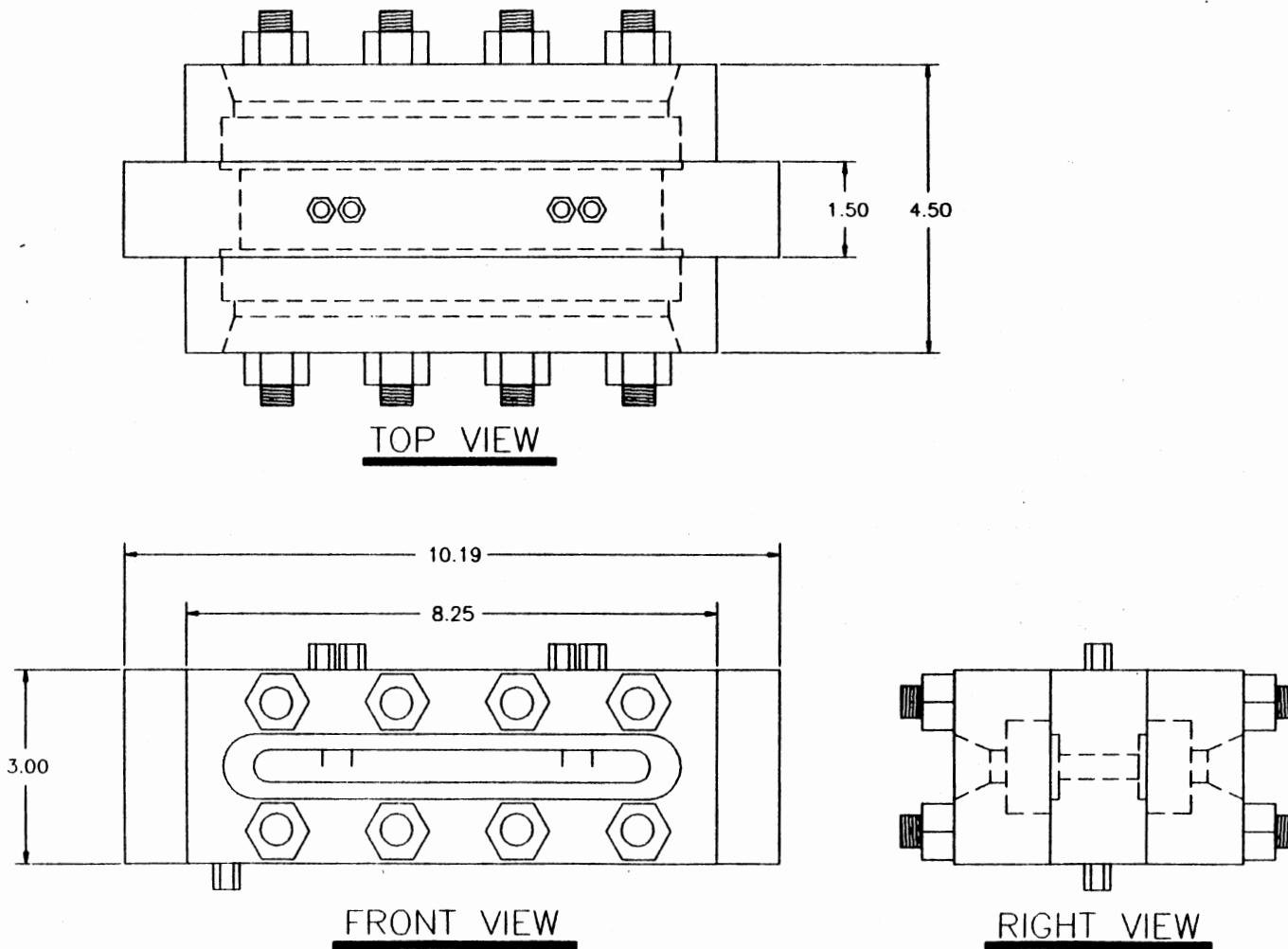


Figure 6. Schematic of the IFT Cell Prototype

needles are equally spaced and each is vertical. This configuration required that a track be constructed to position the point source behind any desired needle at any time. The track and runner were constructed from aluminum with the runner having a hole bored into it with the same diameter as the point source. The track is positioned just behind IFT cell with the point source at the same height as the needle tips. A rod was attached to the runner and extended through the oven wall for manual placement of the light source.

Liquid Density Meter

The liquid density meter (LDMA) cell (model 512), manufactured by Mettler Paar, is used to measure liquid density. Past experience has shown that the liquid DMA cell will not provide period values at low pressures. This may be attributed to the fact that the cell vibrates excessively at low pressures and stable readings are not possible with the employed dampener. The dampener was replaced by a larger carbon steel block about 12" long, 12" high, and 4" thick. Positive results have been seen with the new setup.

Fluid Injection Pump

The fluid injection pump is a Ruska screw pump. During the course of experiments involving mixtures, known amounts of gas were injected into the equilibrium cell. The gas was compressed to a certain pressure and then a small amount was fed to the VLE system. The remaining gas in the pump was then compressed to the original pressure before injection. By reading the volume difference from the pump, an injected volume could then be calculated. A problem in past studies

has been that the room temperature could change as much as 3°F between the time that the injection was made and the time it took to compress the gas to the original pressure and temperature. Therefore, an insulated housing for the pump was made. The housing is basically a wooden box that is fitted with a plexiglass window to view the volume displacement. A thermocouple was attached to the pump cylinder so that temperature changes could be monitored.

CHAPTER IV

AUTOMATION

The purpose of automation in data acquisition and control is to render the process more efficient by utilizing the inherent capabilities of a computer. The choice of equipment to be used in the automation can be simplified by clearly setting the ultimate objectives of the automation process. In upgrading the existing IFT facility, two objectives were developed:

- 1) the automation of temperature, pressure, density, and IFT data acquisition, and
- 2) automation of the temperature control of the constant air bath.

In meeting the above objectives, certain attributes were sought for the automation process:

- 1) the automation equipment must be compatible with the existing facility,
- 2) the automation equipment must be able to acquire data, control the system temperature, run calibration routines, and plot the calibrated data simultaneously, and
- 3) the automation system must be easy to use.

To meet the above objectives, two PC computers and an external I/O modular unit were employed. Additional controller circuit boards needed for temperature control within the oven were designed and

constructed. For the acquisition of drop profiles, video equipment consisting of a camera, monitor, and digitizing PC board were used. Clearly, integration of the separate components of the automation system is the crucial step in the automation process. Therefore, a simple but efficient integration procedure was designed for the automation of the experimental apparatus.

Automation of the existing experimental facility is the result of the interaction of the components mentioned above. As illustrated in Figure 7, the automation scheme undertaken is composed of two parts: first, the acquisition of temperature, pressure, and density, and the control of the temperature in the constant air bath, and second, the capturing of video images of pendant drops for IFT determination. Both parts operate on separate computers and run independently of each other.

Acquisition and Control

The simultaneous acquisition of temperature, pressure, and density, and the control of the system temperature are orchestrated through the integration of a PC, an external I/O unit, control circuit boards, and an acquisition and control software package (see Figure 8). This orchestration is dependent upon the measuring devices available for data transmittal. For data acquisition purposes, the existing measuring equipment was utilized. This included thermocouples and RTD's for measuring temperature, a Sensotec TJE pressure transducer for pressure, and a Mettler Paar DMA 60 density meter for liquid and vapor period values. The measuring device outputs are as follows:

- 1) RTD outputs

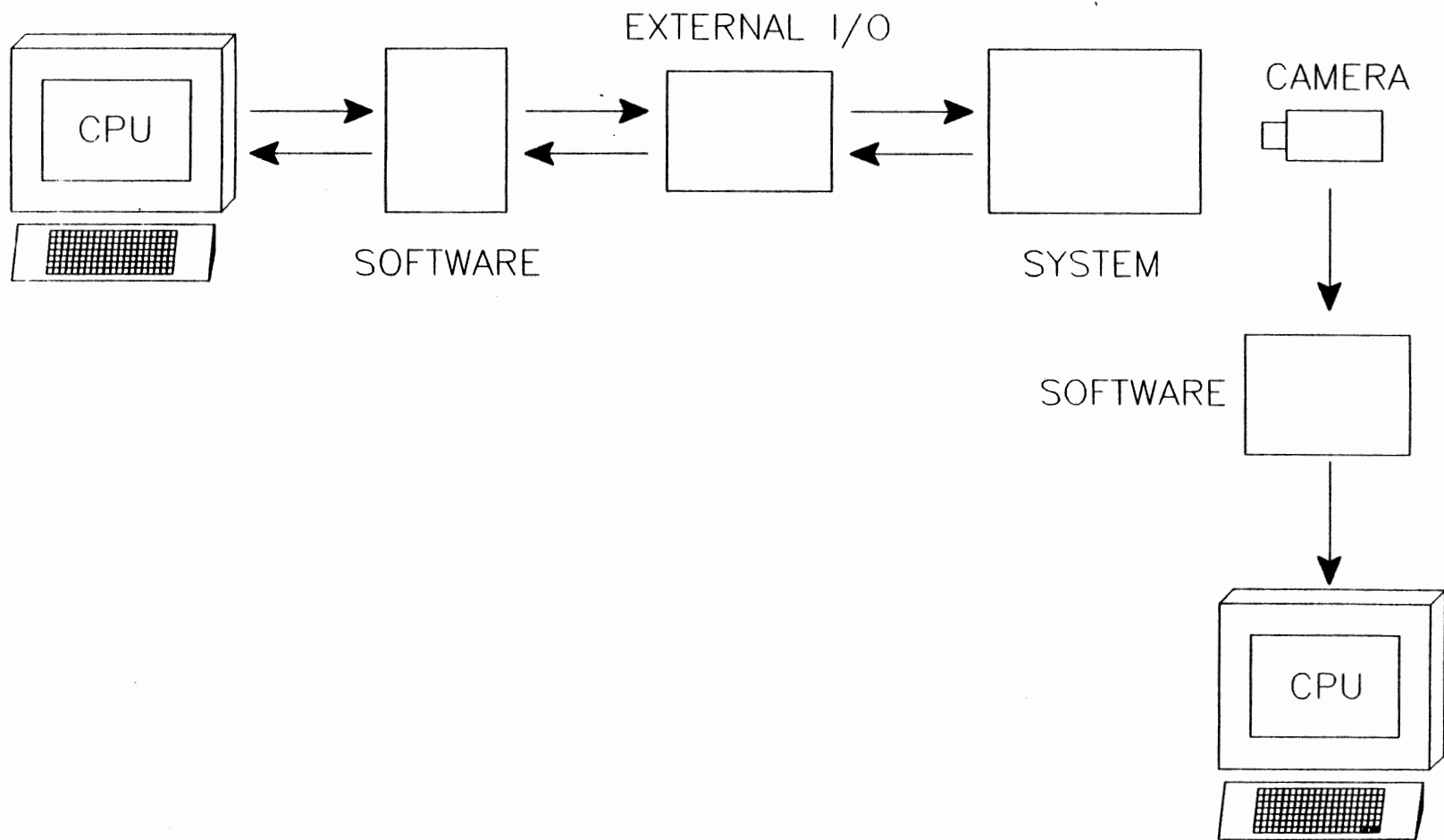


Figure 7. Automated System Overview

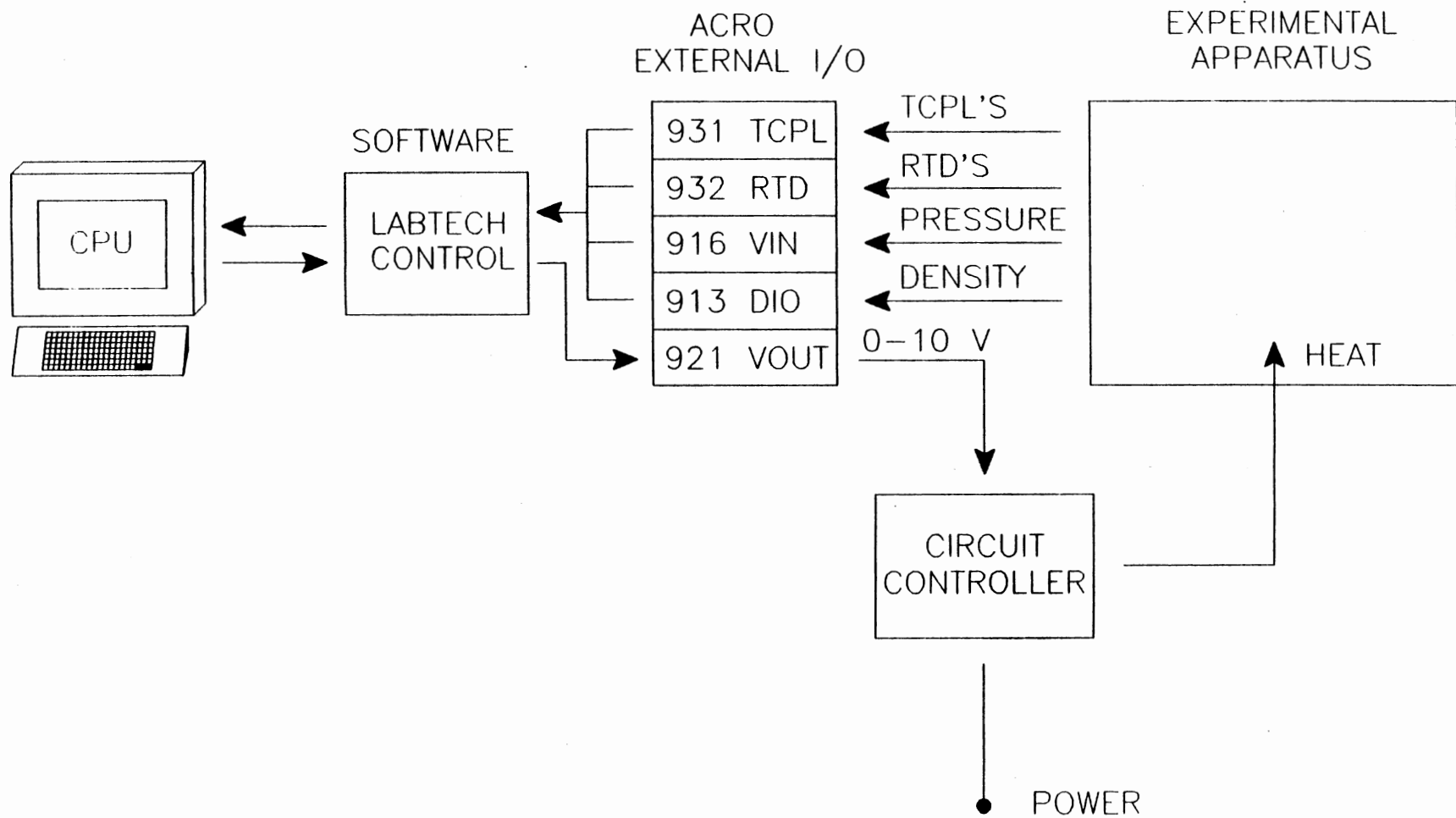


Figure 8. Automated Acquisition and Control Scheme

- 2) thermocouple outputs
- 3) 0-5 volt analog output from the pressure transducer
- 4) 32 bit BCD output from the density meter

The acquisition process involves the use of the external unit to retrieve the system outputs, a computer to interpret and store the raw data from the external unit, and a software package to direct data transmittal. Additionally, the control process is the deployment of circuit controller boards where RTD and thermocouple temperatures are used as input for closed-loop control calculations and the manipulated variable (input voltage to the controller) is transmitted to the controllers via the external I/O unit.

Following is a brief description of the various components needed for data acquisition (excluding the IFT) and temperature control.

Computer

To realize the objectives and desired attributes stated above, we have incorporated a computer that was compatible with our software choices, that could handle a multitasking environment, that could store large amounts of data, and that was fast enough to handle both the data acquisition and control. A Northgate 386 IBM-compatible PC running at 33 MHz with 8 megabytes RAM, a 150 megabyte hard drive, and math coprocessor was purchased. This computer was designated to handle all data acquisition, control, calibration, and graphical representation needs.

External Input / Output Modules

After researching the different options available, the ACRO 900

external I/O modular device was chosen to retrieve the existing measuring device outputs and relay the information to the cpu. The external device is interfaced to the computer via RS-232. This option was selected to protect the computer motherboard from possible system electrical surges and spikes.

The ACRO 900 interface was configured with modules to utilize thermocouples, RTD's, analog, and BCD inputs for data acquisition, and analog outputs for temperature control. The ACRO 900 series employed is equipped with a power and a cpu module. Each of the modules are isolated from each other as well as the individual channels.

The ACRO module 931 provides direct input for up to eight thermocouple sensors. The module features include complete signal conditioning and a built-in cold-junction compensator. The ACRO 931 module utilizes a 16 bit A/D converter for data input conversion. This module was utilized for all thermocouple outputs coming from the experimental system.

The ACRO 932 is an eight channel analog input module designed to be used specifically with 100 Ohm platinum RTD's. The module provides the excitation voltage required for RTD use and handles the signal conditioning, A/D conversion, and linearization and scaling of input signals. The 932 utilizes a 16 bit A/D converter. This module was designated for all RTD outputs measuring the system temperature.

The ACRO 916 module is an analog input and digital I/O device. The module allows for up to eight analog input, eight digital input, and eight digital output lines. The maximum full scale input range for the analog channels is $\pm 20V$. The 916 uses a 12 bit A/D converter for the analog conversion. This module was used to accept the analog

output of the pressure transducer (0-5 V) and convert to a digital signal for the recording of system pressure. None of the digital I/O lines were utilized.

The ACRO 913 module is a multi-channel digital I/O device capable of utilizing up to 60 bidirectional lines, selectable as either input or output. The 913 was used to read the 32 bit BCD output coming from the density meter and relay the period values to the cpu.

The ACRO 921 module provides the analog output required to manipulate additional circuitry used in controlling the system temperature. Eight individual channels are used to provide the 0-10 V output signal which is converted via a 12 bit D/A converter. The module also contains eight digital input and eight digital output lines, none of which are utilized here.

Controllers

As mentioned in Chapter III, three types of heaters are employed to reach a desired set point temperature: a 5 kilowatt heater, a tape heater, and a number of cartridge heaters. The Watlow 900 PID controller that replaced the original controller is used to heat the oven near the desired set point with the 5 kilowatt heater. The tape heater is then utilized to sustain the set point temperature, and the cartridge heaters are employed to alleviate the resulting thermal profile across the oven. The 5 kilowatt heater is not operating when a temperature is sustained, however, the tape and cartridge heaters are. The utilization of the additional heaters requires control circuitry and logic for automation.

A circuit was designed to use the 0-10 V output available from the

ACRO 921 and time proportion a 120 V power supply (see Appendix A). In effect, the circuit supplies a 0 to full power input to the heaters that in previous work, was done manually through Variac voltage regulators. The logic is supplied through software which reads the incoming thermocouple and RTD signals, performs a PI calculation, and returns the calculated output value to the ACRO 921. This value is then sent to the circuit controller board and the output power is regulated. One controller board is employed for the tape heater and four additional boards for the cartridge heaters. After testing this design, an autotransformer was added to the power input of each of the controllers. This allowed for a broader range of heat output and control. In this fashion, temperature control is achieved within the oven.

Microsoft OS/2

During the course of this study, many different software applications are run simultaneously including data acquisition and control, interpretation of data, and graphic representation of data. This combined with word processing needs established a clear requirement for a multitasking environment. Therefore, MS OS/2 was used as the operating system environment.

Labtech Control

Labtech Control is the main software used for data acquisition and control in this work. The software is compatible with both OS/2 and the ACRO 900 series external modules. Labtech Control is a simple to use menu-driven program that allows the user to build input or output

blocks. The software is capable of reading each of the ACRO channels, performing a calibration, using the information as input to a control block, and as a result, control the system. Any or all data may be saved at any time. Its primary use in this study is to record the temperature, pressure, and density output values when desired, and control the system temperature. Since Labtech is OS/2 compatible, the whole program may be put into the background and other software may be utilized simultaneously. See Appendix A for block examples.

Grapher

Golden Software's Grapher was chosen for plotting the acquired data. Although Grapher cannot run under OS/2, it will execute in the DOS compatibility box within OS/2. Grapher utilizes the data files created by the Labtech Control and plots the desired data in specified formats.

A menu-driven program was written to help orchestrate the plotting routines. The program also allows simple maintenance of files and the computer system.

IFT Determination

The acquisition of drop profile images requires separate hardware and software than the above described acquisition process. The image acquisition requires a computer, video camera, monitor, and image digitizing PC board, and software to direct the acquisition. The hardware and software available for image processing require that a DOS environment be used. Therefore, a separate computer was designated for the imaging process.

Computer

Since the imaging process requires a separate computer, a PC Limited 286 IBM-compatible PC running at 12 MHZ with 1 megabyte RAM, a 70 megabyte hard drive, and math coprocessor were obtained. The computer was designated to handle all video processing needs.

Video Equipment

In order to obtain images, a Javelin CCTV B/W camera (model JE2362A) was adapted to the existing Leitz and Wild microscope setup. A 'C' mount was utilized for the interface. A PC Vision plus Frame Grabber card, by Imaging Technology, was purchased and installed into the above computer to provide the ability to digitize any image produced by the camera output. The card utilizes on board memory capable of storing the digitized image and allows for image processing such as image averaging, image subtraction, convolutions, and edge-enhancing routines.

The camera output is fed to the Frame Grabber board and then displayed on a Sony high resolution color monitor (model PVM-1343MD) where all acquired images are viewed.

Imaging Software

Jandel Scientific's JAVA is used to orchestrate the interaction of the camera, board, and monitor. The software provides the tools necessary to acquire an image, display it on the monitor, digitize the image, and store the information on disk. JAVA will also edge-trace the drop profile for the relative X,Y coordinates required for the

determination of IFT.

IFT Routines

A FORTRAN program was created to retrieve the edge-traced data from JAVA and translate the data relative to the drop apex, i.e., to convert the data so that the apex is the origin on a cartesian plot of the profile data. In addition, an estimate of IFT is determined by using the discrete point method described in Chapter II. See Appendix A for the program listing.

Pallas (22) provided a FORTRAN program to take the translated edge-traced coordinates of the drop profile, the measured liquid and vapor density, and the estimate of IFT and determine IFT through a rigorous calculation. The program utilizes a method of rotational discrimination for numerically integrating the differential equation describing the drop profile. The program was adapted for use on the .286 PC.

Integration of Automation Equipment

The integration of the data acquisition and control equipment as well as the video equipment needed for IFT determination is the most crucial step in the automation process. Therefore, a simple but efficient integration procedure was developed for the automation of the IFT facility.

The first step in automating the existing facility, was to (a) install the OS/2 operating environment and the compatible version of Labtech Control and (b) interface the ACRO 900 external I/O device to the computer via RS-232.

The next step, was to facilitate transmission of the system variables, (temperature, pressure, and density period) to the computer. This was accomplished by routing the thermocouple, RTD, pressure transducer output, and density meter output to their corresponding ACRO modules. After this was accomplished, the specially designed controller circuits were interfaced to separate channels of the ACRO 921 module and to heaters within the oven (tape and cartridge). The power input to the controllers was first routed through autotransformers.

Within Labtech Control, blocks were set up to read all thermocouple and RTD signals, the analog output from the transducer, and the BCD output from the density meter. Additional blocks were created for the formation of closed loop control utilized with the tape and cartridge heaters.

Following installation of acquisition and control equipment, their performance to acquire and control was tested. These tests included the comparison temperature measurements made using the thermocouples and RTD's with a specially calibrated resistance thermometer bridge at various temperatures. Observed temperature deviations were accounted for within Labtech. Similarly, the value obtained from the analog output of the pressure transducer was compared to the readout available on the instrument and calibrated within Labtech. The BCD output from the density meter was compared against the available readout and a discrepancy was found. The BCD output was not consistent with the unit readout in the fifth of six decimal places. After observing the discrepancy, the BCD output was deemed incorrect. However, the cost of repairing the unit was not justified for this prototype experiment

and careful attention is needed to assure proper DMA values.

For control purposes, the closed loop control blocks required values for the proportional (P) and integral (I) constants. These constants were calculated by graphical analysis of the heater performance. A step change in the controller voltage input was performed and the resulting temperature dependence was recorded. The plot of temperature versus time for the individual heaters was analyzed by a method described by Smith and Corripio (30), and values for P and I were obtained. These values were then scaled down until no oscillation was observed. See Appendix B for individual step tests and an example analysis and final P and I values.

Once the hardware and software were in place, and the acquisition and control blocks were complete, the system was tested and found to control and acquire as desired. The next step was to add the integration of the video system for IFT determination.

The Video camera was adapted to the Leitz and Wild microscope with an 'LW' clamp and a 2X coupler for better resolution, and the output routed to the Frame Grabber board installed in the 286 PC. The output from the PC Vision board was then routed to the Sony monitor. Following video hardware installation, the JAVA software was installed. The acquisition and analysis of a drop image is done by powering on the camera, monitor, and computer, and then running JAVA. JAVA is used to view live images of the drop until a desired pendant drop is formed. At this time the picture is captured and saved on disk. Later, the drop image can be retrieved and the profile edge-traced. The profile coordinates are then used as input to the program provided by Pallas to determine IFT. A simple image capture and relative X,Y comparison

revealed that an aspect ratio of 0.77 was needed for accurate profile tracing.

Once the IFT hardware and software components were in place, the system was ready for an automated run. See Chapter V for details on automated test runs.

CHAPTER V

EXPERIMENTAL PROCEDURE

This chapter discusses the experimental procedure for measuring the vapor pressure, density, and pendant drop images for pure fluids. This procedure includes apparatus clean-up, calibration of instruments, pressure testing, fluid degassing, and vapor pressure, density, and interfacial tension determination.

The approach used here to study the properties of pure fluids is to create an isothermal environment and let the fluid come to equilibrium at its vapor pressure aided by fluid circulation. Once in equilibrium, the vapor pressure is noted, and the liquid and vapor densities and interfacial tension are determined.

As an overview, the system is cleaned, calibrated, and tested. A pure fluid is then injected and allowed to come to equilibrium at some specified temperature. Relevant data are acquired and the system is then set for a new temperature. Again, once equilibrium is achieved at the new temperature, the relevant data are gathered and the process is repeated. The advantages of such an approach include (1) the ability to study a fluid over a wide range of temperatures and vapor pressures and (2) the convenience of only one initial fluid injection.

The procedures described below are adapted from procedures used previously to measure the properties of multicomponent systems (2-4). In contrast to the previous measurements where high pressure

transducers (up to 10,000 psia) were utilized, the current apparatus employs a 50 psia pressure transducer. Therefore, all testing is conducted below this pressure.

Apparatus Clean-up

The purpose of this step is to clean the experimental apparatus described in chapter III. The procedure is as follows:

- (1) Heat system to about 150°F. Precision in temperature control is not required for this step, thus only the main Watlow controller is utilized.
- (2) Vacuum the system, the injection line, and the fluid injection pump (Ruska pump) through the drain line (see Figure 3).
- (3) Add 250 ml of n-C₅ to the buret above the Ruska Pump.
- (4) Isolate the system from the Ruska pump by the shut-off valve.
- (5) Open the buret containing the n-C₅ to the Ruska pump and displace the piston until approximately 100 ml fill the pump.
- (6) Isolate the buret from the Ruska pump and the system from the vacuum. Open the shut-off valve connecting the Ruska pump and the system.
- (7) Displace the n-C₅ into the system and isolate the Ruska pump from the system.
- (8) Open the CO₂ line leading to the Ruska pump and carefully open the cylinder and regulate CO₂ pressure to just under 50 psia.
- (9) Slowly open the shut-off valve between the Ruska pump and the system and add CO₂ to the system until the pressure reaches

about 40 psia. This step may have to be repeated as the CO_2 dissolves into the n-C₅.

- (10) Allow the system to circulate vapor for about 15 minutes and then switch to liquid circulation for about 15 minutes. Repeat steps 2-10 as desired. Depending on the fluid previously in the system, the procedure can be repeated anywhere from three to six times.

System Calibration

In order to obtain reliable data, all system instruments must be calibrated. This includes the thermocouples, the RTD's, the pressure transducer, the liquid and vapor DMA cells, and the imaging system. As mentioned before, The apparatus is to be used over a range of temperatures and therefore, an accounting for the effect of temperature on the various instruments is essential.

The thermocouples and the RTD's are calibrated by placing each of the probes into an aluminum block made to accommodate the various probes in a common thermal environment. A Minco resistance thermometer bridge utilizing an NBS calibrated probe is also inserted into the block. The temperature within the oven is then allowed to stabilize at intervals within the range of the future operating temperatures. At each temperature, the Minco probe, thermocouples, and RTD's are recorded and the deviations determined.

The pressure transducer is temperature compensated and located just outside the oven wall. Experience has shown no significant deviation in calibration with temperature. Therefore, a simple dead weight calibration is performed on the system. In this study, the

transducer was calibrated over a 0-50 psia range and a linear deviation was found, as shown in Appendix C.

Once the temperature and pressure calibrations have been completed, the liquid and vapor density meters need to be calibrated at various temperatures and pressures. The density meters are calibrated using air and water as reference fluids. Periods of oscillation for each fluid at various pressures are fitted to the equation:

$$\tau = A + BP + CP^2 + DP^3 \quad (11)$$

where

τ = period of oscillation of density meter

P = pressure of the fluid

A,B,C,D = fitting constants

Interpolation between the reference fluids is then used to convert the density meter count of a given sample to a density by the following equation:

$$\rho = K(\tau^2 - \tau_w^2) + \rho_w \quad (12)$$

where

$$K = (\rho_a - \rho_w) / (\tau_a^2 - \tau_w^2) \quad (13)$$

τ_a, τ_w = density meter count for air and water

ρ, ρ_a, ρ_w = sample, air, and water densities

The density meter is calibrated as follows:

- (1) Choose a priori the isotherms to be studied.
- (2) Bring system temperature to the selected temperature.

Precise temperature control is essential.

- (3) Vacuum the system after making sure the system is clean.
- (4) Inject about 45 psia of air into the system.
- (5) Circulate in vapor mode for 10 minutes.
- (6) Shut off circulation and wait till density period stabilizes.
Drain some air out (amount depends on pressure range) and repeat until the lower end of operating pressure is reached.
- (7) Repeat steps 4-6 for liquid DMA readings.
- (8) Achieve the new desired temperature and repeat steps 4-7.
- (9) When the air calibration is complete, repeat steps 2-8 with water.

Experience has shown that the density meters deviate significantly with temperature and need to be calibrated at each isotherm of interest. No attempt was made to develop a calibration over a specified temperature range. See Appendix C for calibrations at 120°F.

The imaging system does not require calibration; however, the aspect ratio needs to be determined for each optical configuration. As long as the lenses and digitizing board do not change, the aspect ratio will not change.

The aspect ratio, defined as the ratio of the Y-coordinate magnification to the X-coordinate magnification, is determined by taking an object of known dimensions and recording the image using the camera and the JAVA software. The image is then digitized and analyzed. The ratio given by dividing the Y-distance by the X-distance is calculated as the aspect ratio. In this study, numerous objects were used to determine the aspect ratio and a value of 0.77 was found. This ratio is taken in account by setting FGAR = 0.77 in the AUTOEXEC.BAT file on the computer running the JAVA software. No other

calibrations are needed for the imaging process.

Pressure Testing

The need for a leak-free system, especially when dealing with sub-atmospheric pressures is very important. The pressure test is accomplished by vacuuming the system and then injecting helium at room temperature to a pressure above the maximum operating pressure. After helium injection, the pressure is monitored over a 12 hour period. If a pressure loss does occur, a high sensitive helium leak detector is used to locate the sources of the leak. Once the system holds pressure at room temperature, the temperature is raised to the maximum operating temperature and the pressure test redone. If leaks do occur, the detector is employed again until the system is leak-free.

Data Acquisition

After completion of the system calibration and the integrity check, the study may begin. The experiment is begun by vacuuming the system and setting the Watlow controller at a setpoint approximately 5°F under the true desired temperature. After about 2 hours, the tape and cartridge heaters are employed via Labtech Control. At this point, the fluid under study is degassed and injected. The degassing is accomplished by one of two ways: (a) If the vapor pressure of the fluid at the system temperature is greater than atmospheric, then the fluid must be pumped in using the Ruska pump. The degassing is accomplished by adding the fluid to the burret above the Ruska pump and a vacuum is pulled over the top. The injection is made by releasing the vacuum over the burret and withdrawing about 100 ml of the fluid into

the Ruska pump. The system is then isolated from vacuum, and the fluid is injected. (b) If the vapor pressure is less than atmospheric, then the fluid is degassed in a separate flask by pulling a vacuum over it. The flask top is closed and joined to a separate buret connected directly to the system and is evacuated. Once the buret is under vacuum the flask is opened and fills the buret. The system is then isolated from its vacuum and the buret is allowed to drain into the system. For a 100 ml sample, multiple injections are required.

Once the fluid is injected, the system is set on vapor circulation until equilibrium temperature and pressure are reached at which point the circulation is stopped and the VDMA period is monitored until constant.

The data point is taken by putting Labtech Control into the OS/2 background and running the WDT program. The WDT program is menu driven and has data point acquisition as a selection. Once this is selected, the user is prompted for the system name and whether this is a LDMA or VDMA reading. The program then collects one data point, and converts the period reading to density and records the raw and the calibrated data. The WDT program then allows the user to view graphical representation of all data collected or return back to Labtech Control.

After the vapor phase measurement is taken, the system is switched to liquid circulation for about 30 minutes and the above procedure for the vapor is repeated for the liquid. Once the liquid density measurement is completed, the pendant drop image is captured using the following procedure:

- (1) Power up the camera and JAVA.
- (2) Recirculate liquid

- (3) Stop the circulation, close the shut-off valve, and close all but one of the isolating valves. Then, slowly close the needle valve until a drop just forms on the tip of the needle. If the drop is too small or exhibits very little curvature then another needle needs to be selected. Repeat the procedure until a desired needle size is found. (See Figure 9 for valve configuration.)
- (4) Close needle valve until drop is pendant. Experimentation with pendant drops is necessary to obtain best results.
- (5) Capture several pendant images of the drops with JAVA. (The system may be set at its new temperature at this time if desired.)
- (6) Edge trace the images starting from the upper left corner of the needle.
- (7) Run the IFT program, which first translates the data so that the apex is at 0,0 and calculates an initial guess for the IFT by using the discrete point method. User input for liquid and vapor density is required and is taken from the WDT program. The IFT program, as discussed earlier, uses the routine supplied by Pallas to calculate the IFT using rotational discrimination.
- (8) Repeat steps 1 through 7 at next temperature.

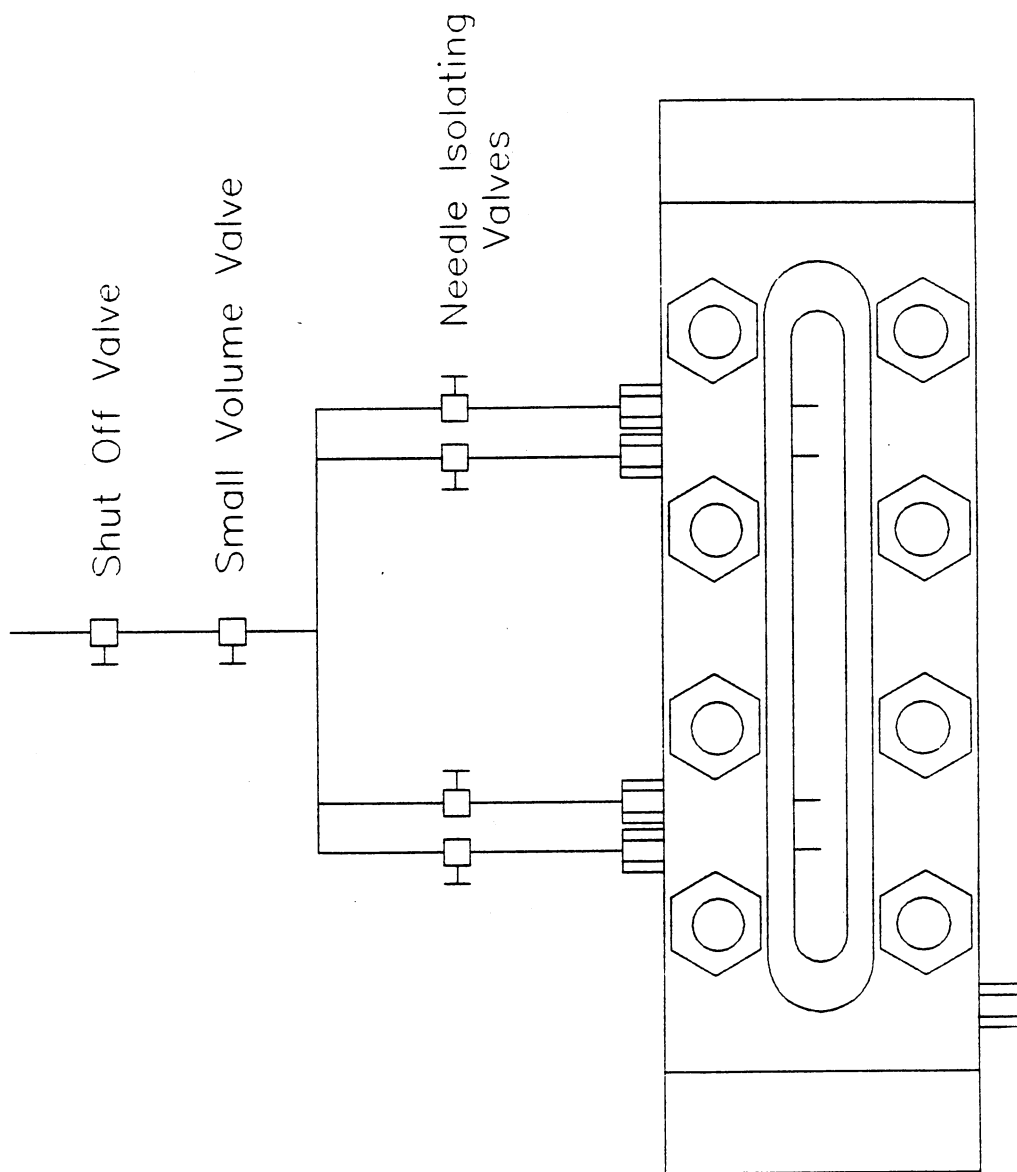


Figure 9. IFT Valve Configuration

CHAPTER VI

EXPERIMENTAL RESULTS AND DISCUSSION

Experimental test runs with n-pentane (n-C₅) at 120°F were performed to establish the reliability of the automated apparatus. The n-C₅ was supplied by J. T. Baker with a reported purity of 99.7%. Vapor pressure, liquid and vapor densities, and interfacial tension were determined and compared with available literature data.

Experimental Data

Tables I and II present the experimental vapor pressure, vapor and liquid densities, and interfacial tension data obtained during the test runs. The expected uncertainty of the experimental data, detailed in Appendix D, is estimated as:

| | |
|-----------------|------------|
| Temperature: | 0.1°F |
| Vapor Pressure: | 0.1 psia |
| Densities: | 0.001 g/cc |
| IFT: | 3% |

A comparison of experimental measurements made for the vapor pressure and phase densities with literature values for n-C₅ at 120°F is presented in Table I. The data agree well with the literature values with the exception of vapor density which exhibits a slightly larger disagreement with the literature. The experimental vapor

TABLE I
 COMPARISON OF EXPERIMENTAL AND LITERATURE
 VALUES FOR VAPOR PRESSURE AND DENSITY OF
 n-C₅ AT 120°F

| Property | # Exptl. Run | Exptl. Results | Lit. Values |
|-----------------------|--------------------|-------------------|----------------|
| Vapor Pressure (psia) | 1 | 22.4 | |
| | 2 | 22.4 | 22.35 (31) |
| | 3 | 22.4 | 22.29 (32) |
| Liquid Density (g/cc) | 1 | 0.5974 | |
| | 2 | 0.5970 | 0.5969 (31) |
| | 3 | 0.5969 | 0.5964 (33) |
| Vapor Density (g/cc) | 1 | 0.0056 | |
| | 2 | 0.0054 | |
| | 3 | 0.0054 | 0.004395 (31) |

TABLE II
 COMPARISON OF EXPERIMENTAL AND LITERATURE VALUES FOR $\gamma/\Delta\rho$
 FOR n-C₅ AT 120°F

| Image # | Needle O.D. (in.) | $\gamma/\Delta\rho$, (dyne-cm)/(g/cm ³) | | % Difference* | |
|---------|----------------------|--|------------------------|---------------|---------|
| | | Discrete Method | Profile Integration | Discrete | Profile |
| 1 | 0.02 | 20.99 (12.42)** | 20.25 (11.98) | -0.99 | -4.48 |
| 2 | 0.02 | 21.54 (12.75) | 20.76 (12.28) | 1.60 | -2.08 |
| 3 | 0.02 | 21.92 (12.97) | 21.30 (12.60) | 3.40 | 0.47 |
| 4 | 0.02 | 20.80 (12.31) | 20.87 (12.35) | -1.89 | -1.56 |
| 5 | 0.028 | 21.80 (12.90) | 21.68 (12.83) | 2.83 | 2.26 |
| 6 | 0.028 | 21.93 (12.96) | 21.89 (12.95) | 3.44 | 3.25 |
| 7 | 0.028 | 21.13 (12.50) | 21.36 (12.64) | -0.33 | 0.75 |
| 8 | 0.028 | 22.07 (13.06) | 21.65 (12.81) | 4.10 | 2.12 |
| 9 | 0.0355 | 21.30 (12.60) | 21.33 (12.62) | 0.47 | 0.61 |
| 10 | 0.0355 | 21.26 (12.58) | 21.19 (12.54) | 0.28 | -0.05 |
| 11 | 0.0355 | 21.22 (12.56) | 21.57 (12.76) | 0.09 | 1.75 |
| 12 | 0.0355 | 21.19 (12.54) | 21.13 (12.50) | -0.05 | -0.33 |
| | average | 21.43 (12.68) | 21.25 (12.57) | | |
| | standard deviation | 0.41 (0.24) | 0.46 (0.27) | | |

* % difference is calculated using the literature value with each of the methods.

Literature values (34): $\gamma/\Delta\rho = 21.20$, $\gamma = 12.56$

** The corresponding γ values in dyne-cm

densities are 0.001 to 0.0012 g/cc high. The higher vapor density may be attributed to the increased pressure induced by the mechanical pump (further details are given in the discussion section).

A comparison of experimental and literature IFT values is shown in Table II. $\gamma/\Delta\rho$ (along with γ values) are presented since $\gamma/\Delta\rho$ is determined directly from the image analysis. The table also compares $\gamma/\Delta\rho$ using the discrete method (used in previous studies) and the complete profile integration method, which employs the rotational discrimination procedure provided by Pallas (22). While the average $\gamma/\Delta\rho$ from the numerical integration is closer to the literature value, the standard deviations of both methods are nearly the same; moreover, the IFT values determined by the discrete method encompass the literature value. The maximum percent difference observed for both methods, including all needle sizes, is about 5%.

Table II also shows that the different needle sizes lead to different IFT estimates. In fact, by comparing the percent difference for each of the needles, the IFT values obtained using the 0.0355 inch diameter needle are closest to the literature value and the most reproducible. The ability to a priori determine the optimum needle size for a given VLE system would depend on initial estimates for the IFT. For experimental systems where no data have been reported, the process for finding the optimum needle size might prove to be a trial-and-error procedure.

The value for $\gamma/\Delta\rho$ was determined by taking a number of pendant drop images on different needle sizes and extracting the profile through the edge tracing technique. The edge tracing was performed a number of times on each image and found to give identical results for a

given image. Each drop image was edge traced, translated with origin at the apex, and analyzed with the discrete method in a matter of minutes. Figure 10 shows a typical edge traced data set. As can be seen in this figure, most of the data are redundant (typical edge traces contain around 1000 points) which slows the numerical integration considerably. Therefore, the number of data points for the profile coordinates was reduced prior to integration. Thorough testing of the integration procedure revealed that about 250 profile coordinates are needed to accurately describe the drop profile with little or no loss in precision. Once the data set was reduced, the coordinates required additional translation and conversion from pixel values to distances in centimeters for input to the program provided by Pallas. Figure 11 shows the same data set used in Figure 10 with the data translated and converted.

The numerical integration program of Pallas provides for an additional translation and rotation of the experimental profile coordinates. This alleviates errors due to camera misalignment and small deviations in the verticality of the needle. The experimental profile is rotated and translated according to the following equations:

$$X_i = (X_i^{\text{exp}}/M_x - X_0)\cos\theta + (aZ_i^{\text{exp}}/M_x - Z_0)\sin\theta \quad (14)$$

$$Z_i = (aZ_i^{\text{exp}}/M_x - Z_0)\cos\theta - (X_i^{\text{exp}}/M_x - X_0)\sin\theta \quad (15)$$

where (X_0, Z_0) is the coordinate of the apex and θ is the angle of rotation. The objective function used in the numerical integration is

$$Q = \sum_{i=1}^m r_i^2 \quad (16)$$

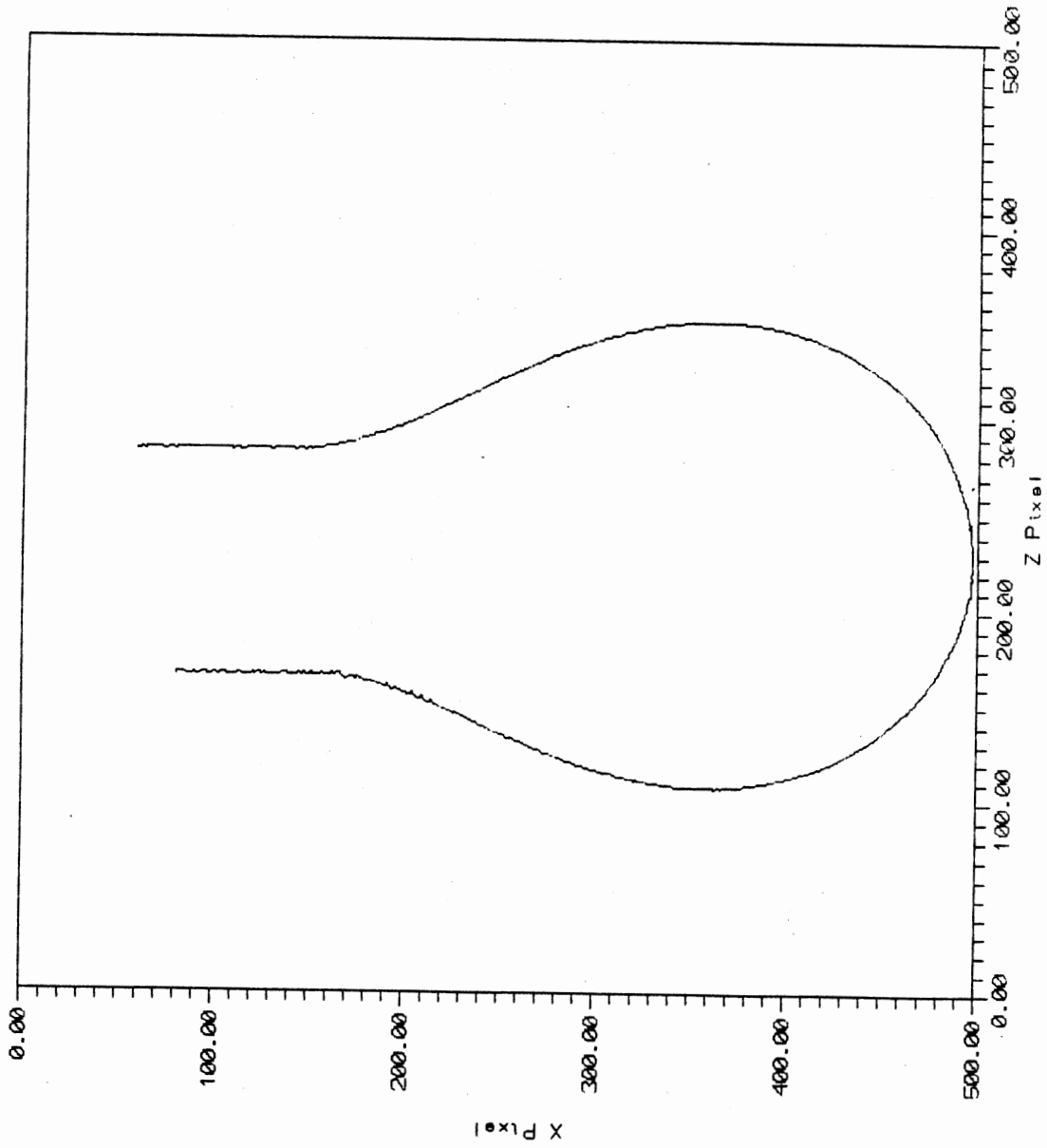


Figure 10. Typical Edge Traced Drop Profile

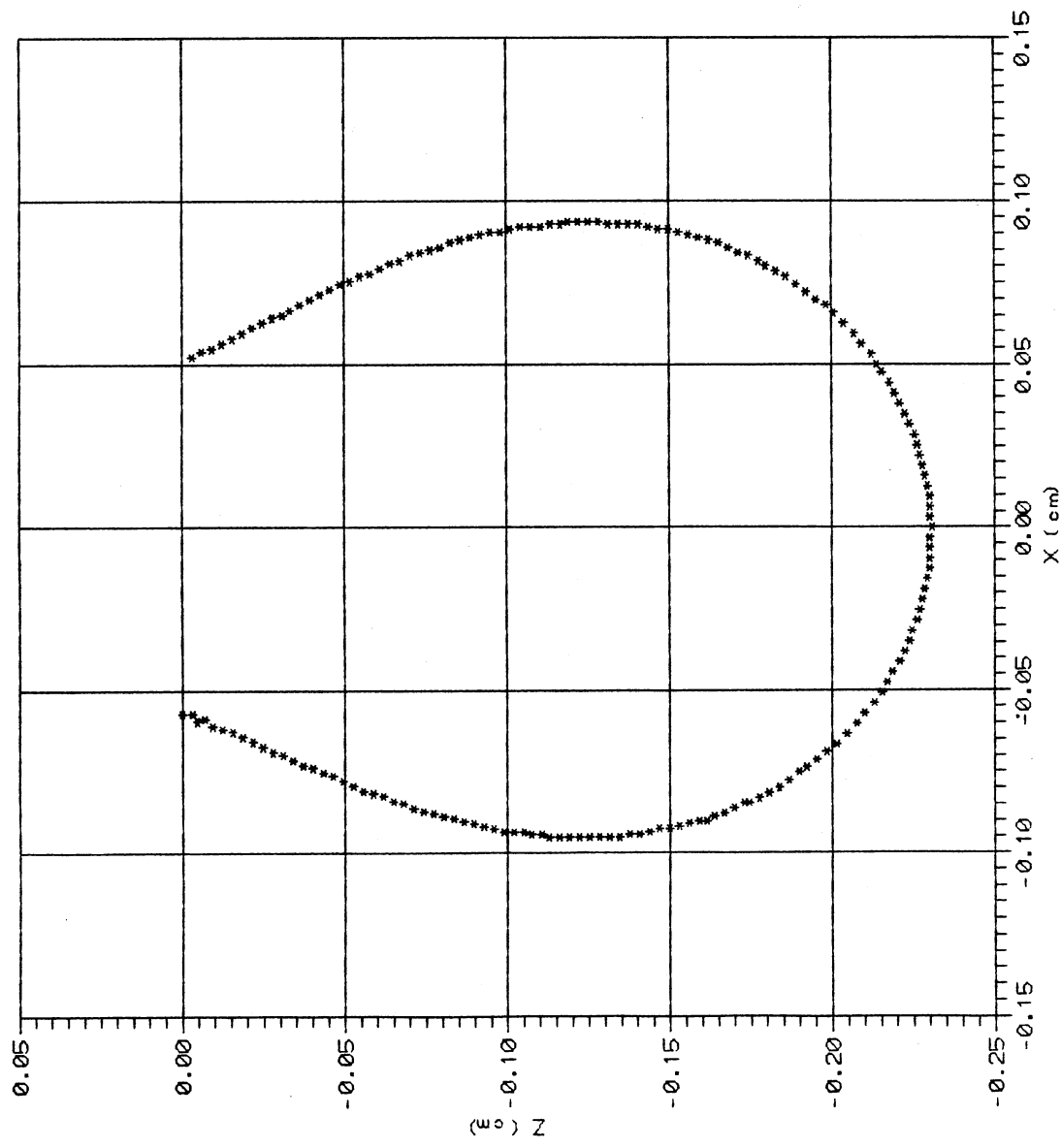


Figure 11. Typical Translated and Converted Drop Profile

where,

$$r_i = \pm[(X(s_i) - X_i)^2 + (Z(s_i) - Z_i)^2]^{1/2} \quad (17)$$

Equations 16 and 17 define the objective function, Q, as the sum of the squared residuals r_i , where r_i equals the distance between the transformed data point (X_i, Z_i) and the corresponding closest point on the calculated drop shape $(X(s_i), Z(s_i))$ (22). Figure 12 shows a plot of the integrated profile residuals for the 0.0355 inch needle. The plot indicates that the experimental drop profile is slightly off the vertical axis, however, the calculated residuals are small and well within the estimated imprecision of the IFT measurement.

Discussion

The automated data acquisition and control system operated smoothly. The acquisition of raw data, the instantaneous interpolation of density from the acquired density cell period, and the storage of the results presented no problems. The temperature control also worked well with the ability to control any probe location to within 0.1°F. However, a few minor difficulties were encountered during the test run.

The circulation of liquid n-C₅ within the two phase environment creates a temperature profile within the system. Specifically, the VDMA cell heats up and the LDMA cell cools down. This phenomenon can be explained by the fact that the magnetic pump acts as an evaporator near the LDMA cell at the bottom of the pump and a condenser near the VDMA cell at the top of the cell. The phenomenon was verified by circulating vapor and compressed liquid separately. In both cases, no variation in temperature was observed. The problem was overcome by

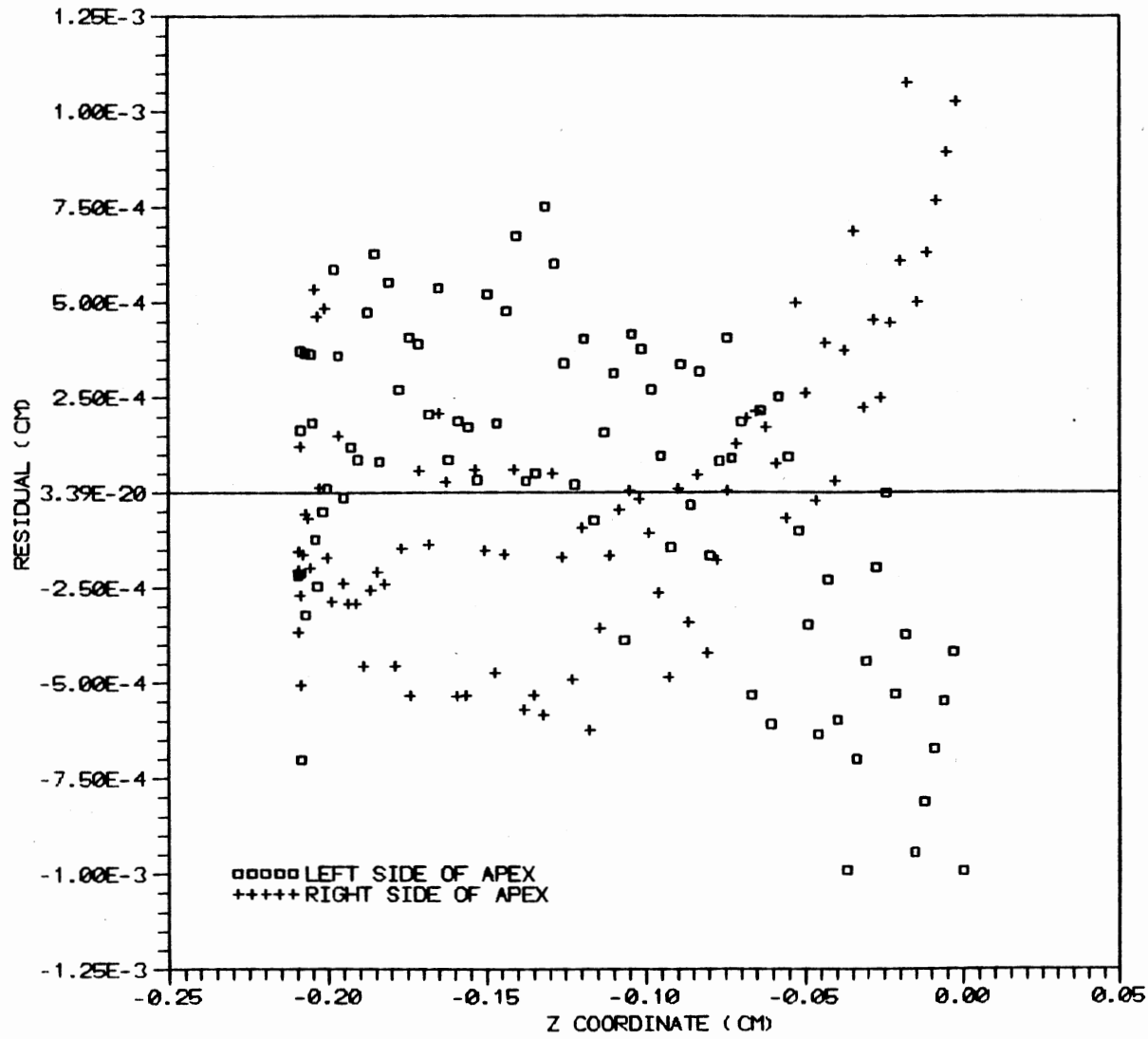


Figure 12. Integrated Profile Residual for the 0.0355 Inch Needle.

circulating the two phase system and waiting for the temperature to regain stability at the desired set point.

Utilizing a 12 bit A/D converter, the ACRO module 916 is used to read the 0-5 volt analog output from the pressure transducer and pass the converted digital variable to the computer via RS-232. The 12 bit A/D converter allows for a resolution of 0.1 psia with the existing 0-50 psia pressure transducer. This resolution, however, deteriorates for the 0-3000 psia pressure transducer (used for high pressure studies) and becomes about 6 psia. To obtain a better pressure resolution, two solutions are proposed:

- 1) acquisition of a 17 bit A/D converter capable of 0.2 psia resolution with the 3000 psia transducer, or
- 2) design of a circuit to amplify the transducer output to accommodate the possible ± 20 volt input range to the 916 ACRO module. This will produce a resolution of about 0.7 psia with the 3000 psia transducer.

The new IFT cell prototype operated successfully with the current system. However, higher pressures and good vacuum are difficult to achieve due to small leaks in the cell. Pendant drops are a little difficult to form due to recoiling of the drops even after the upstream valves have been closed. This may be attributed to the large volume of fluid in the circulation lines running from the needles to the shut off valve of the IFT cell. To avoid this problem, it was necessary to insure that only liquid was present in the lines directly above the needles; a task accomplished by initially injecting enough liquid to fill the PVT cell 3/4 full.

The automated analysis of the drop images works very well. Each

drop image was edge traced and $\gamma/\Delta\rho$ determined by both the discrete method and the complete integration of the drop profile. However, preliminary results indicate no significant gain in precision was realized when using the complete profile integration approach. Further testing is needed to contrast the characteristics of the two techniques.

The Labtech Control functioned properly within the OS/2 operating environment but failed periodically when other DOS programs were run in the DOS box. The failure, however, did not occur with the acquisition or analysis of data, but with certain application programs dealing with file maintenance that conflicted with the OS/2 operating environment.

Overall, the automation of the existing IFT facility was a success. The results show that temperature control is very easily achieved to within 0.1°F, barring disruption of temperature control in the LDMA and VDMA cells caused by the fluid recirculation pump. The IFT cell prototype operated well, especially when compared with the previously used cell. The preliminary testing of the apparatus provides good evidence on its reliability. While precise measurement for vapor pressure, phase densities, and interfacial tensions are obtained within the experimental uncertainty, further testing is required to render a firmer assessment.

CHAPTER VII

CONCLUSIONS AND RECOMMENDATIONS

Conclusions

An existing vapor-liquid equilibrium experimental apparatus designed for the measurement of phase densities and interfacial tension of pure fluids and mixtures was automated. The automation provides for computerized data acquisition and temperature control as well as instantaneous analysis of the raw data. The data acquisition and control was mostly accomplished using a single computer operating in an OS/2 environment which allows for computer multitasking. The determination of IFT, however, was done using a separate computer which utilized an image digitizing card, and analysis software not compatible with the OS/2 operating system.

Physical modifications were made also to the system, the major change being the design and construction of a new IFT cell. A working prototype of the IFT cell was constructed and successfully tested. The new IFT design alleviates the need for O-rings and moving parts which have hindered past work.

Although time constraints did not permit a thorough evaluation of the experimental apparatus at different temperatures, a test run was conducted on n-C₅ at 120°F to establish the reliability of the apparatus.

The result of the automation and the replacement of the IFT cell

have shown very positive results, specifically: 1) The ability to achieve a temperature to within 0.1°F of the set point is now accomplished within four hours; thus avoiding a trial-and-error procedure which may take days, and 2) the new cell, coupled with the image digitizing system, work extremely well. A pendant drop image can now be digitized and analyzed in less than ten minutes. The new IFT system reduces both the time needed to analyze the pendant drop images and the potential for human error in the analysis.

Recommendations

Although the system performed well, several items are suggested to further improve this facility.

- 1) More tests, using different chemicals over a wide range of temperatures, should be conducted. This will utilize the system to its full potential and uncover other possible problems not encountered in this study.
- 2) Controlling the temperature of the various units within the oven is relatively simple using the existing heaters, probes, and Labtech Control. However, the temperature variations experienced by the VDMA and LDMA cells, which are mechanically induced by the magnetic pump, may not be easy to eliminate. A more detailed study is therefore recommended to establish the appropriate means for eliminating the induced temperature profile.
- 3) Problems still exist for OS/2 and care must be taken when operating in this environment. The data acquisition and control software work well in the environment but are prone to

failure when certain DOS programs are run simultaneously. It is recommended that future application software purchases have OS/2 in mind; OS/2 can only run one DOS application at a time and multitasking is impossible if OS/2 software is not utilized.

- 4) Although the acquisition of the DMA period is complete, the signal sent from the density meter is still incorrect in the fifth of six decimal places. It is recommended that the density meter be repaired before the next study is undertaken.

LITERATURE CITED

1. Girault, H. H., D. J. Schiffrin, and B. D. V. Smith, "Drop Image Processing for Surface and Interfacial Measurements," *J. Electroanal. Chem.*, 137, 207-217 (1982).
2. Gasem, K. A. M., K. B. Dickson, P. B. Dulcamara, N. Nagarajan, and R. L. Robinson, Jr., "Equilibrium Phase Compositions, Phase Densities, and Interfacial Tensions for CO₂ + Hydrocarbon Systems. 5. CO₂ + n-Tetradecane," *J. Chem. Eng. Data*, 34, 191-195 (1989).
3. Nagarajan, N. and R. L. Robinson, Jr., "Equilibrium Phase Compositions, Phase Densities, and Interfacial Tensions for CO₂ + Hydrocarbon Systems. 2. CO₂ + n-Decane," *J. Chem. Eng. Data*, 31, 168 (1986).
4. Hsu, J. C., N. Nagarajan, and R. L. Robinson Jr., "Equilibrium Phase Compositions, Phase Densities, and Interfacial Tensions for CO₂ + Hydrocarbon Systems. 1. CO₂ + n-Butane," *J. Chem. Eng. Data*, 30, 485 (1985).
5. Laplace, P. S., "Mecanique Celeste," Duprat, Paris, (1806).
6. Bashforth, F., and J. C. Adams, "An Attempt to Test the Theories of Capillary Action," University Press, Cambridge, England, (1883).
7. Andreas, J. M., E. A. Hauser, and W. B. Tucker, "Boundary Tension by Pendant Drops," *J. Phys. Chem.*, 42, 1001 (1938).
8. Girault, H. H., D. J. Schiffrin, and B. D. V. Smith, "The Measurement of Interfacial Tension of Pendant Drops Using a Video Image Profile Digitizer," *J. Colloid Interf. Sci.*, Vol. 101, No. 1, 257-266 (1984).
9. Maze, C., and G. Burnet, "Modifications of a Non-Linear Regression Technique Used to Calculate Surface Tension from Sessile Drops," *Surface Sci.* 24, 335 (1971).
10. Huh, C. and R. L. Reed, "A Method for Estimating Tensions and Contact Angles from Sessile and Pendant Drop Shapes," *J. Colloid Interf. Sci.*, 91, 472 (1983).
11. Butler, J. N., and B. H. Bloom, "A Curve Fitting Method for Calculating Interfacial Tension from the Shape of a Sessile Drop," *Surface Sci.*, 4, 1 (1966).

12. Patterson, R. E., and S. Ross, "The Pendant Drop Method to Determine Surface or Interfacial Tensions," *Surface Sci.*, 81, 451 (1979).
13. Fordham, S., "On the Calculation of Surface Tension from Measurements of Pendant Drops," *Proc. Roy. Soc. (London)*, A194, 1 (1948).
14. Niederhauser, D. O., and F. E. Bartell, "Report of Progress - Fundamental Research on the Occurrence and Recovery of Petroleum, 1948-1949," American Petroleum Institute, Baltimore, Md., 114 (1950).
15. Dulcamara, P. B., "Interfacial Tension for Carbon Dioxide or Light Hydrocarbons in Hydrocarbon Solvents: Experimental Data and Correlations," Thesis, Oklahoma State University, Stillwater, OK., (1987).
16. Mills, O. S., "Tables for use in the measurement of interfacial tensions between liquids with small densities differences," *British Journal of Applied Physics*, Vol. 4 (1953).
17. Roe, Ryong-Joon, V. L. Bacchetta, and P. M. G. Wong, "Refinement of Pendant Drop Method for the Measurement of Surface Tension of Viscous Liquid," *J. Phys. Chem.*, Vol 71, No. 13, 4190-4193 (1967).
18. Winkel, D., "Theoretical Refinement of the Pendant Drop Method for Measuring Surface Tensions," *J. Phys. Chem.*, 69, 348 (1965).
19. Stauffer, C. E., "The Measurement of Surface Tension by the Pendant Drop Technique," *J. Phys. Chem.*, 69, 1933 (1965).
20. Ambwani, D. S., and T. Fort, "Surface and Colloid Science," Vol II, 93-119, Plenum Press, New York (1979).
21. Rotenburg, Y., L. Boruvka, and A. W. Neuman, "Determination of Surface Tension and Contact Angle from the Shapes of Axisymmetric Fluid Interfaces," *J. Colloid Interf. Sci.*, Vol 93, No. 1 (1983).
22. Jennings, J. W. and N. R. Pallas, "An Efficient Method for the Determination of Interfacial Tensions from Drop Profiles," *Langmuir*, Vol 4, No. 4, 959-967 (1988).
23. Law, V. J., and R. H. Fariss, "Transformational Discrimination for Unconstrained Optimization," *Ind. Eng. Chem. Fundam.*, 11, 154 (1972).
24. Eckman, D. P., "Automatic Process Control," John Wiley and Sons, (1962).
25. Vernov, N. I., V. G. Lisienko, D. B. Zheltyshev, and I. G. Koval'chuk, "Microprocessor-Based Control Unit for Vibrating Measuring Instruments," *Measurement Techniques*, 31, 11, 1101-1104 (1989).

26. Okada, M., M. Uematsu, and K. Watanabe, "Orthobaric Liquid Densities of Trichlorofluoromethane, Dichlorodifluoromethane, Chlorodifluoromethane, 1,1,2-Trichlorotrifluoroethane, 1,2-Dichlorotetrafluoroethane, and of the Azeotropic mixture of (Chlorodifluoromethane + Chloropentafluoroethane) Between 203 and 463 K," *J. Chem. Thermodynamics*, 18, 527-543 (1986).
27. Maezawa, Y., H. Sato, and K. Watanabe, "Saturated Liquid Densities of HCFC 123 and HFC 134a," *J. Chem. Engr. Data*, 35, 225-228 (1990).
28. Doyle, P. J. and B. J. Carroll, "A Improved and Semi-Automated Version of the Drop Volume Technique for Interfacial Tension Measurement," *J. Phys. E: Sci. Instr.*, Vol. 22, No. 7, 431-433 (1989).
29. Anastasiadis, S. H., I. Gancarz, and J. T. Koberstein, "Interfacial Tension of Immiscible Polymer Blends: Temperature and Molecular Weight Dependence," *Macromolecules*, 21, 2980-2987 (1988).
30. Smith, C. A., and A. B. Corripio, "Principles and Practice of Automatic Process Control," John Wiley and Sons (1985).
31. Timmermans, J., "Physico-Chemical Constants of Pure Organic Compounds," Vol. 1, Interscience, N. Y. (1950).
32. Vargaftic, N. B., "Tables on the Thermophysical Properties of Liquids and Gases," 2nd Ed., Hemisphere Publishing Corp., Washington D.C. (1975).
33. TRC Thermodynamic Tables: Hydrocarbons, Thermodynamics Research Center, Texas A&M University.
34. Jeffries, T. O., "Surface Tension of Ether and Pentane," *J. Chem. Physics*, 23, 1730 (1955).
35. Vasserman, A. A., Ya. Z. Kazavchinskii, and V. A. Rabinovich, "Thermophysical Properties of Air and Air Components," Keter Press, Jerusalem (1971).
36. ASME Steam Tables, 5th Ed., ASME Committee of Properties of Steam, New York (1983).

APPENDIX A

AUTOMATION INTEGRATION

In the process of automating the system, Labtech Control was utilized for data acquisition and control. The following block formats are typical examples of the ones used in this work.

TABLE A.1
TYPICAL BLOCK SETUP FOR A THERMOCOUPLE

| | |
|--|----------------|
| Number of Function Blocks [0..373] | 23 |
| Current Block(s) [n or n..m] | 1 |
| Block Type | [Thermocouple] |
| Tag Name | PVT TC1 |
| Block Units | F |
| Device | [4: ACRO 931] |
| Point/Channel Number [1..8] | 1 |
| Temperature Scale | [Fahrenheit] |
| Thermocouple Type | [J] |
| Scale Factor | 1.000 |
| Offset Constant | 0.000 |
| Hi-Hi Alarm Limit | 300.000 |
| Hi Alarm Limit | 300.000 |
| Lo Alarm Limit | 0.000 |
| Lo-Lo Alarm Limit | 0.000 |
| Alarm Deadband | 0.100 |
| Alarm Processing | [Annunciate] |
| Buffer Size | 100 |
| Number of Iterations | 1 |
| Number of Stages [1..4] | 1 |
| Sampling Period, sec. | 1.000 |
| Stage Duration, sec. [0.0..1.0E+08] | 1.00E+08 |
| Start/Stop Method | [Immed.] |
| Trigger Block or Key | 1 |
| Trigger Pattern to AND [0..255] | 1 |
| Trigger Pattern to XOR [0..255] | 0 |
| Time Delay, sec. [0.0..1.0E+08] | 0.000 |
| Analog Trigger Value | 0.000 |
| Analog Trigger Polarity | [High] |
| Number of Samples to Save (Pretrigger) | 0 |

TABLE A.2
TYPICAL BLOCK SETUP FOR A RTD

| | |
|--|---------------|
| Number of Function Blocks [0..373] | 23 |
| Current Block(s) [n or n..m] | 5 |
| Block Type | [RTD] |
| Tag Name | Tape RTD1 |
| Block Units | F |
| Device | [4: ACRO 932] |
| Point/Channel Number [1..8] | 1 |
| Temperature Scale | [Fahrenheit] |
| RTD Type | [American] |
| User Defined Constant: R0 | 100.000 |
| Alpha | 3.85E-03 |
| Delta | 1.450 |
| C4 | 1.20E-03 |
| Scale Factor | 1.000 |
| Offset Constant | 0.000 |
| Hi-Hi Alarm Limit | 300.000 |
| Hi Alarm Limit | 300.000 |
| Lo Alarm Limit | 0.000 |
| Lo-Lo Alarm Limit | 0.000 |
| Alarm Deadband | 0.100 |
| Alarm Processing | [Annunciate] |
| Buffer Size | 100 |
| Number of Iterations | 1 |
| Number of Stages [1..4] | 1 |
| Sampling Period, sec. | 1.000 |
| Stage Duration, sec. [0.0..1.0E+08] | 1.00E+08 |
| Start/Stop Method | [Immed.] |
| Trigger Block or Key | 1 |
| Trigger Pattern to AND [0..255] | 1 |
| Trigger Pattern to XOR [0..255] | 0 |
| Time Delay, sec. [0.0..1.0E+08] | 0.000 |
| Analog Trigger Value | 0.000 |
| Analog Trigger Polarity | [High] |
| Number of Samples to Save (Pretrigger) | 0 |

TABLE A.3
TYPICAL BLOCK SETUP FOR AN ANALOG OUTPUT

| | |
|-------------------------------------|-----------------|
| Number of Function Blocks [0..373] | 23 |
| Current Block(s) [n or n..m] | 8 |
| Block Type | [Analog Output] |
| Tag Name | AOUT PVT |
| Block Units | V |
| Device | [4: ACRO 921] |
| Point/Channel Number [1..8] | 1 |
| Scale Factor | 1.000 |
| Offset Constant | 0.000 |
| Hi-Hi Alarm Limit and Output Clamp | 10.000 |
| Hi Alarm Limit | 10.000 |
| Lo Alarm Limit | 0.000 |
| Lo-Lo Alarm Limit and Output Clamp | 0.000 |
| Alarm Deadband | 0.100 |
| Alarm Processing | [Annunciate] |
| Loop | [Closed] |
| Loop Gain (P) | 11.250 |
| Loop Reset (I) | 3.80E-03 |
| Loop Rate (D) | 0.000 |
| Loop Setpoint | 120.000 |
| Setpoint Block (0=none) | 0 |
| Start in Automatic Mode | [Yes] |
| Starting Value for Output | 0.000 |
| Input Block Number | 1 |
| Buffer Size | 100 |
| Number of Iterations | 1 |
| Number of Stages [1..4] | 1 |
| Sampling Period, sec. | 1.000 |
| Stage Duration, sec. [0.0..1.0E+08] | 1.00E+08 |
| Start/Stop Method | [Immed.] |
| Trigger Block or Key | 1 |
| Trigger Pattern to AND [0..255] | 1 |
| Trigger Pattern to XOR [0..255] | 0 |
| Time Delay, sec. [0.0..1.0E+08] | 0.000 |
| Analog Trigger Value | 0.000 |
| Analog Trigger Polarity | [High] |

TABLE A.4

TYPICAL BLOCK SETUP FOR AN ANALOG INPUT

| | |
|--|----------------|
| Number of Function Blocks [0..373] | 23 |
| Current Block(s) [n or n..m] | 13 |
| Block Type | [Analog Input] |
| Tag Name | PRESSURE |
| Block Units | Psia |
| Device | [4: ACRO 916] |
| Point/Channel Number [1..8] | 1 |
| Input Range | [± 20 V] |
| Scale Factor | 1.000 |
| Offset Constant | 0.000 |
| Hi-Hi Alarm Limit | 20.000 |
| Hi Alarm Limit | 20.000 |
| Lo Alarm Limit | -20.000 |
| Lo-Lo Alarm Limit | -20.000 |
| Alarm Deadband | 0.100 |
| Alarm Processing | [Annunciate] |
| Buffer Size | 100 |
| Number of Iterations | 1 |
| Number of Stages [1..4] | 1 |
| Sampling Period, sec. | 1.000 |
| Stage Duration, sec. [0.0..1.0E+08] | 1.00E+08 |
| Start/Stop Method | [Immed.] |
| Trigger Block or Key | 1 |
| Trigger Pattern to AND [0..255] | 1 |
| Trigger Pattern to XOR [0..255] | 0 |
| Time Delay, sec. [0.0..1.0E+08] | 0.000 |
| Analog Trigger Value | 0.000 |
| Analog Trigger Polarity | [High] |
| Number of Samples to Save (Pretrigger) | 0 |

TABLE A.5
TYPICAL BLOCK SETUP FOR A DIGITAL INPUT

| | |
|--|-----------------|
| Number of Function Blocks [0..373] | 23 |
| Current Block(s) [n or n..m] | 14 |
| Block Type | [Digital Input] |
| Tag Name | DMA BCD1 |
| Block Units Device | [4: ACRO 913] |
| Point/Channel Number [1..8] | 1 |
| Select Bit? | [No] |
| Bit Number [1..8] | 1 |
| Hi-Hi Alarm Limit | 100.000 |
| Hi Alarm Limit | 100.000 |
| Lo Alarm Limit | 0.000 |
| Lo-Lo Alarm Limit | 0.000 |
| Alarm Deadband | 0.100 |
| Alarm Processing | [Annunciate] |
| Buffer Size | 100 |
| Number of Iterations | 1 |
| Number of Stages [1..4] | 1 |
| Sampling Period, sec. | 1.000 |
| Stage Duration, sec. [0.0..1.0E+08] | 1.00E+08 |
| Start/Stop Method | [Immed.] |
| Trigger Block or Key | 1 |
| Trigger Pattern to AND [0..255] | 1 |
| Trigger Pattern to XOR [0..255] | 0 |
| Time Delay, sec. [0.0..1.0E+08] | 0.000 |
| Analog Trigger Value | 0.000 |
| Analog Trigger Polarity | [High] |
| Number of Samples to Save (Pretrigger) | 0 |

TABLE A.6
TYPICAL BLOCK SETUP FOR A CALCULATION

| | |
|--|--------------|
| Number of Function Blocks [0..373] | 23 |
| Current Block(s) [n or n..m] | 18 |
| Block Type | [Calculated] |
| Tag Name | BCD1 |
| Block Units | |
| Operation | [BCD(X)] |
| X Input Block | 14 |
| Y Input Block | 1 |
| Z Input Block | 1 |
| Parameter, r | 0.000 |
| Scale Factor | 1.00E-06 |
| Offset Constant | 0.000 |
| Hi-Hi Alarm Limit | 100.000 |
| Hi Alarm Limit | 100.000 |
| Lo Alarm Limit | 0.000 |
| Lo-Lo Alarm Limit | 0.000 |
| Alarm Deadband | 0.100 |
| Alarm Processing | [Annunciate] |
| Buffer Size | 100 |
| Number of Iterations | 1 |
| Number of Stages [1..4] | 1 |
| Sampling Period, sec. | 1.000 |
| Stage Duration, sec. [0.0..1.0E+08] | 1.00E+08 |
| Start/Stop Method | [Immed.] |
| Trigger Block or Key | 1 |
| Trigger Pattern to AND [0..255] | 1 |
| Trigger Pattern to XOR [0..255] | 0 |
| Time Delay, sec. [0.0..1.0E+08] | 0.000 |
| Analog Trigger Value | 0.000 |
| Analog Trigger Polarity | [High] |
| Number of Samples to Save (Pretrigger) | 0 |

The circuits used for controlling the oven temperature were designed by Jimmy Bryson at Oklahoma State University after consultation with the author. Five identical circuits were housed in a single metal box with the circuit power supply also enclosed. The unit basically contains 10 inlet lines for the 0-10 volt controlling input, 5 sockets for power input and 5 for power output to the heaters. The Circuit diagram is shown in Figure A.1.

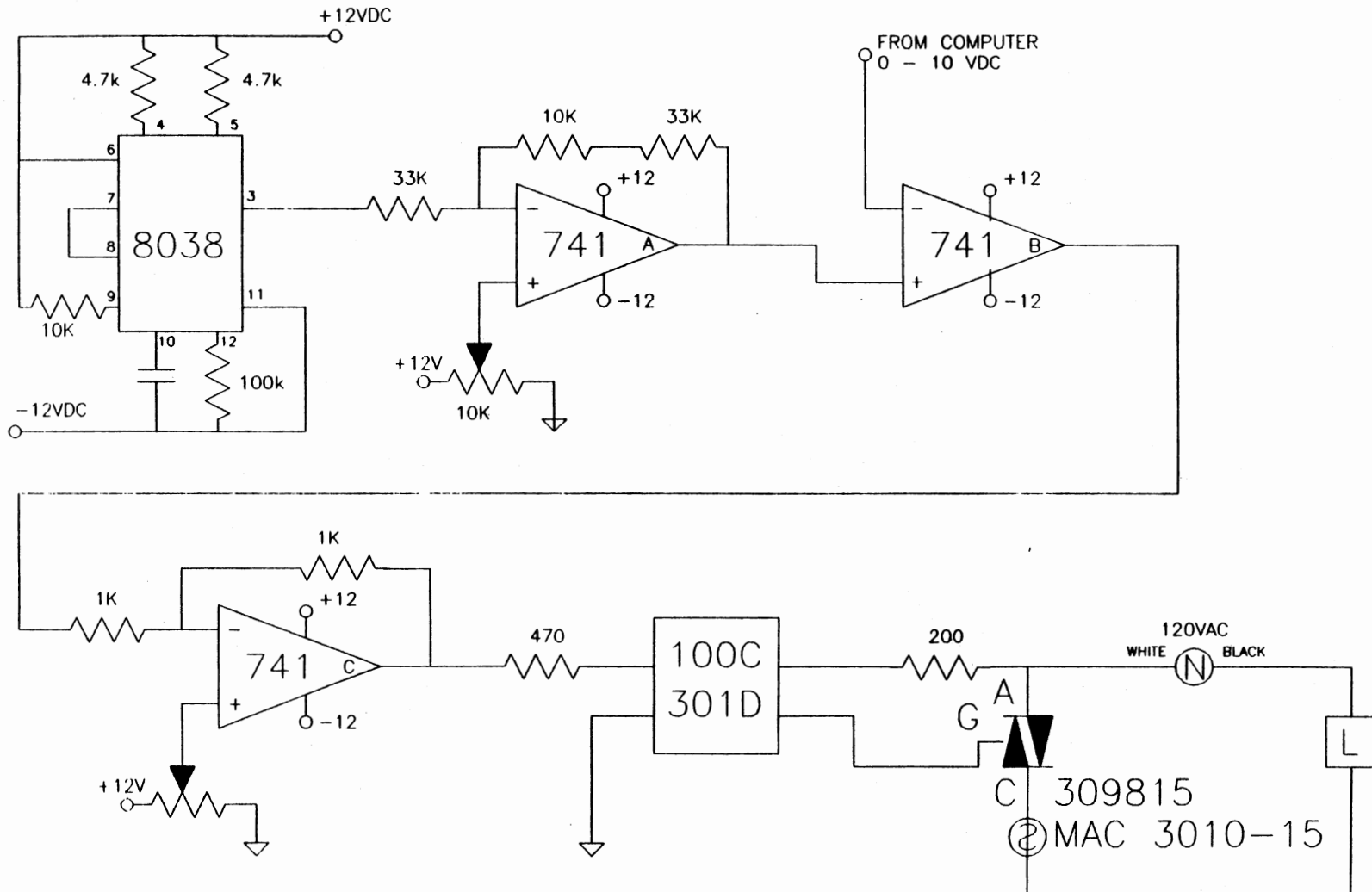


Figure A.1 Schematic for Controller Circuit

Three programs were used in the automation of the experimental facility.

- 1) TRANS.FOR - this program was designed to translate the edge-traced data produced from JAVA and estimate IFT for use in the program provided by Pallas (DROP.FOR).
- 2) DROP.FOR - this program was provided by Pallas (22) which utilizes a rotational discrimination approach to pendant drop determination. The program was originally written for a VAX system but was adapted to run on the PC's used in this work.
- 3) WDT.FOR - this program was written to orchestrate data recording, calibration, and graphical representation.

The TRANS and WDT programs are listed below.

```

C     TRANS.FOR
C
C     KURTIS V. ROUSH
C
C     LOCATE APEX, XMIN, XMAX, CALCULATE De AND Ds FROM
C     DROP PROFILE DATA, AND ESTIMATE IFT
C
C     THE PROGRAM ASSUMES THAT THE EDGE IS TRACED STARTING FROM THE
C     LEFT SIDE.  THE RIGHT SIDE MUST EXTEND HIGHER OR EVEN TO THE
C     LEFT SIDE.  THE PROGRAM ASSUMES THAT THE MONITOR IS TURNED ON
C     END.
C
C     VARIABLES:
C
C     X -      X COORDINATE
C     Y -      Y COORDINATE
C     DIAXL -  X COORDINATE OF LEFT SIDE OF NEEDLE
C     DIAXR -  X COORDINATE OF ROGHT SIDE OF NEEDLE
C     DIAMAG - DIAMETER OF MAGNIFIED NEEDLE IN PIXELS
C     APEX -   INTEGER VALUE REPRESENTING ARRAY VALUE OF THE APEX
C     APEXX -  X COORDINATE OF THE APEX
C     APEXY -  Y COORDINATE OF THE APEX
C     XMIN -   FAR LEFT X VALUE
C     XMAX -   FAR RIGHT X VALUE
C     DE -     MAXIMUM WIDTH OF DROP
C     DSL -    X COORDINATE ON LEFT SIDE OF DROP A DISTANCE DE FROM
C             THE APEX
C     DSR -    X COORDINATE ON RIGHT SIDE OF DROP A DISTANCE DE FROM
C             THE APEX
C     DS -     THE WIDTH OF THE DROP A DISTANCE DE FROM THE APEX
C     NDIA -   ACTUAL NEEDLE DIAMETER IN INCHES
C     LIQDEN - DENSITY OF THE LIQUID PHASE
C     VAPDEN - DENSITY OF THE VAPOR PHASE
C     DELROE - DIFFERENCE IN LIQUID AND VAPOR DENSITY
C     S -      RATIO DE/DS
C     H -      FACTOR DEPENDENT ON S
C     IFT -    CALCULATED IFT USING DISCRETE POINT METHOD
C
C*****
C
C     IMPLICIT REAL (A-Z)
C     DOUBLE PRECISION X(2000),Y(2000)
C     INTEGER N,NPTS,APEX,START,END
C     CHARACTER*28 FILE1,FILE2
C     CHARACTER*11 FIL
C
C     WRITE(6,*) 'INPUT DATA FILE NAME'
C     READ(5,'(A7)') FIL
C     FILE1='C:\NC5\TRACE\'//FIL//'.DAT'
C     FILE2='C:\NC5\TRACE\'//FIL//'.EDG'
C     OPEN(UNIT=8, FILE=FILE1, STATUS='OLD')
C     OPEN(UNIT=9, FILE=FILE2, STATUS='UNKNOWN')
C
C ***** HACK OFF FIRST 10 POINTS DUE TO ERROR IN GUESSING EDGE

```

```

C
    DO 100 N=1,10
        READ(8,*)
    100 CONTINUE
C
C ***** READ REST OF DATA POINTS AND CORRECT FOR IMAGE BEING
SIDEWAYS C
    N=0
    20 CONTINUE
        N=N+1
        READ(8,*,END=30) Y(N),X(N)
        Y(N)= -Y(N) + 1000.0
        GOTO 20
C
    30 NPTS=N-1
C
C ***** HACK OFF RIGHT SIDE OF TRACE ABOVE LEFT SIDE
C
    N=NPTS
    40 IF(Y(N).LE.Y(1))THEN
        NPTS=N
        GOTO 50
    ENDIF
    N=N-1
    GOTO 40
C
    50 CONTINUE
C
C ***** CALCULATE MAGNIFIED DIAMETER USING AVERAGE OF TOP 10 LEFT
AND TOP 10 RIGHT X COORDINATES
C
    DIAXL=0.0
    DO 110 N=1,10
        DIAXL=DIAXL+X(N)
    110 CONTINUE
    DIAXL=DIAXL/10.0
C
    DIAXR=0.0
    DO 120 N=NPTS,NPTS-9,-1
        DIAXR=DIAXR+X(N)
    120 CONTINUE
    DIAXR=DIAXR/10.0
C
    DIAMAG=DIAXR-DIAXL
C
C ***** LOCATE APEX
C
    YMIN2Q=1000.00
    DO 130 N=1,NPTS
        IF(Y(N).LT.YMIN2Q) THEN
            YMIN2Q=Y(N)
            Y2Q=N
        ENDIF
    IF(Y(N).EQ.YMIN2Q) THEN

```

```

                YMIN3Q=Y(N)
                Y3Q=N
            ENDIF
130 CONTINUE
C
    APEX=INT((Y3Q+Y2Q)/2)
    APEXX=X(APEX)
    APEXY=Y(APEX)
C
C    TRANSFORMS COORDINATES RELATIVE TO THE APEX (0,0)
C
    DO 135 N=1,NPTS
        X(N)=X(N)-APEXX
        Y(N)=Y(N)-APEXY
REM        WRITE(9,133) x(n), y(n)
133    FORMAT(10x,F10.4,10x,F10.4)
135 CONTINUE
C
C ***** LOCATE MINIMUM X
C
    XMIN=1000
    DO 140 N=1,APEX
        IF(X(N).LT.XMIN) THEN
            XMIN=X(N)
        ENDIF
140 CONTINUE
C
C ***** LOCATE MAXIMUM X
C
    XMAX=0.0
    DO 150 N=APEX,NPTS
        IF(X(N).GT.XMAX) THEN
            XMAX=X(N)
        ENDIF
150 CONTINUE
C
C ***** CALCULATE De AND Ds
C
    DE=XMAX-XMIN
    YS=Y(APEX)+DE
    N=0
160 N=N+1
    IF(Y(N).LE.YS) THEN
        DSL=X(N)
        GOTO 161
    ENDIF
    GOTO 160
161 CONTINUE
    N=NPTS
170 N=N-1
    IF(Y(N).LE.YS) THEN
        DSR=X(N)
        GOTO 171
    ENDIF

```

```

GOTO 170
171 CONTINUE
DS=DSR-DSL
C
C ESTIMATE GAMMA/DELTA RHO (dyne-cm)/(g/cc)
C
WRITE(*,*)'Enter needle diameter in inches'
READ(*,*) NDIA
DE=DE*NDIA/DIAMAG
DS=DS*NDIA/DIAMAG
DE=DE/39.37
DS=DS/39.37
C
S=DS/DE
H=1/(0.31470 * S**(-2.62529))
C
IFT=1.0E6*(9.79777*DE**2.0)/H
WRITE(*,1000) IFT
1000 FORMAT(2X,'GAMMA/DELTA RHO = ',F7.3,' (dyne-cm)/(g/cc)')
IFT=IFT*0.592505
WRITE(*,1010) IFT
1010 FORMAT(2X,'GAMMA = ',F7.3,' (dyne-cm)')
C
C PREPARE DATA FILE FOR PALLAS PROGRAM
C
C REMOVE DATA ENCOMPASSING NEEDLE
C
I=2
200 IF(ABS(X(1)-X(I)).LE.10.0) THEN
    I=I+1
    GOTO 200
ENDIF
START=I
C
I=NPTS-1
210 IF(Y(I).GE.Y(START)) THEN
    I=I-1
    GOTO 210
ENDIF
END=I
C
C TRANSLATE THE DATA SO Y(1), THE HIGHEST POINT, IS AT X,0
C
YORIGIN=Y(START)
DO 300, I=START,END
    Y(I)=Y(I)-YORIGIN
300 CONTINUE
C
C CONVERT DATA FROM PIXELS TO CENTIMETERS
C
NDIA=NDIA*30.48/12.0
DO 400, I=START,END
    X(I)=X(I)*NDIA/DIAMAG
    Y(I)=Y(I)*NDIA/DIAMAG

```

```
        WRITE(9,500) X(I), Y(I)
400    CONTINUE
500    FORMAT(10X,F10.6,10X,F10.6)
      STOP
      END
```

```

*
*   WDT.FOR ... (Whole Damn Thing)
*
*   INTERFACE TO INTEGER*2 FUNCTION SPAWNLP [C,VARYING] (MODE)
*   INTEGER*2 MODE
*   END
*   INTERFACE TO INTEGER*2 FUNCTION SYSTEM [C] (STRING[REFERENCE])
*   CHARACTER*1 STRING
*   END
*   INTEGER*2 SYSTEM
*
*   CALL MAINMENU
*   I=SYSTEM('CLS'C)
*   STOP
*   END
*****
*   SUBROUTINE MAINMENU
*****
*   CHARACTER*3 BEGH,RC
*   CHARACTER*1 BEGX(3), ENDH
*   INTEGER CHOICE
*   INTEGER*2 SPAWNLP,SYSTEM
*   EQUIVALENCE (BEGH,BEGX)
*
*   BEGX(1)=CHAR(19)
*   BEGX(2)=CHAR(255)
*   BEGX(3)=CHAR(1)
*   ENDH=CHAR(1)
*
*   1  WRITE(*,*) BEGH, 'MOUSE, YES', ENDH
*     WRITE(*,*) BEGH, 'USE, MAIN.AID', ENDH
*     WRITE(*,*) BEGH, 'EXIT, RET=C', ENDH
*     WRITE(*,*) BEGH, 'EXIT, RET=V, ESC=A, FKO=H', ENDH
*     WRITE(*,*) BEGH, 'MENU, RC', ENDH
*
*   READ(*,5) RC
*   5  FORMAT(A3)
*     IF(RC.EQ.'ESC') GOTO 7
*   7  CONTINUE
*     READ(*,10) CHOICE
*   10 FORMAT (I2)
*
*     IF(CHOICE.EQ.001) CALL PLOT
*     IF(CHOICE.EQ.002) THEN
*       I=SPAWNLP(0, LOC('E:\\SYSTEM\\GRAPH\\GRAPHER'C),
* *     LOC('E:\\SYSTEM\\GRAPH\\GRAPHER'C), INT4(0))
*     ENDIF
*     IF(CHOICE.EQ.003) THEN
*       I=SPAWNLP(0, LOC('C:\\XTGOLD\\XTGOLD'C),
* *     LOC('C:\\XTGOLD\\XTGOLD'C), INT4(0))
*     ENDIF
*     IF(CHOICE.EQ.004) THEN
*       I=SYSTEM('CLS'C)
*       CALL SAMPLE

```

```

ENDIF
IF(CHOICE.EQ.005) GOTO 1000
GOTO 1
1000 CONTINUE
RETURN
END
*****
SUBROUTINE PLOT
*****
*   This routine deletes data files in the graph directory and *
*   replaces them with the desired data files.  It then gives *
*   options for presenting the data. *
*****
CHARACTER*3 BEGH,RC
CHARACTER*1 BEGX(3), ENDH
CHARACTER*7 NAME
CHARACTER*30 FILE1,FILE2,FILE3,FILE4,FILE5,FILE6
INTEGER CHOICE,DATE,TIME
INTEGER*2 SPAWNLP
INTEGER*2 SYSTEM
EQUIVALENCE (BEGH,BEGX)
*
*   REPLACES DATA FILES IN GRAPHER DIRECTORY WITH DESIRED DATA
*
I=SYSTEM('CLS'C)
I=SYSTEM('DEL E:\\SYSTEM\\GRAPH\\RAW.DAT'C)
I=SYSTEM('DEL E:\\SYSTEM\\GRAPH\\VAP.DAT'C)
I=SYSTEM('DEL E:\\SYSTEM\\GRAPH\\LIQ.DAT'C)
*
WRITE(*,*)
WRITE(*,*)
WRITE(*,*)
WRITE(*,*)
WRITE(*,*)
WRITE(*,*)
WRITE(*,*)
WRITE(*,*) ' HERE ARE AVAILABLE DATA SETS'
WRITE(*,*) ' '
I=SYSTEM('DIR E:\\SYSTEM\\DATA\\*.RAW'C)
5 WRITE(*,*) ' '
WRITE(*,*) ' ENTER SYSTEM OF INTEREST EX. <CO2>'
WRITE(*,*) ' ENTER <R> TO RETURN TO MAIN MENU'
READ(5, '(A7)') NAME
IF(NAME.EQ.'R') GOTO 1001
*
FILE1='E:\\SYSTEM\\DATA\\'//NAME//'.RAW'
FILE2='E:\\SYSTEM\\DATA\\'//NAME//'.LIQ'
FILE3='E:\\SYSTEM\\DATA\\'//NAME//'.VAP'
FILE4='E:\\SYSTEM\\GRAPH\\RAW.DAT'
FILE5='E:\\SYSTEM\\GRAPH\\LIQ.DAT'
FILE6='E:\\SYSTEM\\GRAPH\\VAP.DAT'
*
*   CHECK TO SEE IF FILES EXIST
*   (IF .RAW DOES NOT, .LIQ & .VAP WILL NOT)
*

```



```

OPEN(UNIT=8, ERR=16, FILE=FILE1, STATUS='OLD')
GOTO 17
16 WRITE(*,*) ' THIS DATA FILE IS NOT AVAILABLE'
GOTO 5
17 OPEN(UNIT=9, FILE=FILE2, STATUS='OLD')
OPEN(UNIT=10, FILE=FILE3, STATUS='OLD')
OPEN(UNIT=11, FILE=FILE4, STATUS='NEW')
OPEN(UNIT=12, FILE=FILE5, STATUS='NEW')
OPEN(UNIT=13, FILE=FILE6, STATUS='NEW')
*
20 READ(8,*,END=30)DATE, TIME, TPVT, TIFT, TVDMA, TLDMA, TTAPE, PRES,
* PERIOD
WRITE(11,1000)DATE, TIME, TPVT, TIFT, TVDMA, TLDMA, TTAPE, PRES,
* PERIOD
GOTO 20
30 READ(9,*,END=40)DATE, TIME, TPVT, TIFT, TVDMA, TLDMA, TTAPE, PRES,
* DEN
WRITE(12,1000)DATE, TIME, TPVT, TIFT, TVDMA, TLDMA, TTAPE, PRES,
* DEN
GOTO 30
40 READ(10,*,END=50)DATE, TIME, TPVT, TIFT, TVDMA, TLDMA, TTAPE, PRES,
* DEN
WRITE(13,1000)DATE, TIME, TPVT, TIFT, TVDMA, TLDMA, TTAPE, PRES,
* DEN
GOTO 40
1000 FORMAT(2I12,6F12.2,F12.6)
*
50 CONTINUE
CLOSE(8)
CLOSE(9)
CLOSE(10)
CLOSE(11)
CLOSE(12)
CLOSE(13)
*
* GRAPH MENU FOR OPTIONS TO PLOT
*
BEGX(1)=CHAR(19)
BEGX(2)=CHAR(255)
BEGX(3)=CHAR(1)
ENDH=CHAR(1)
*
60 WRITE(*,*) BEGH, 'MOUSE, YES', ENDH
WRITE(*,*) BEGH, 'USE, PLOT.AID', ENDH
WRITE(*,*) BEGH, 'EXIT,RET=C', ENDH
WRITE(*,*) BEGH, 'EXIT,RET=V,ESC=A,FKO=H', ENDH
WRITE(*,*) BEGH, 'MENU,RC', ENDH
*
READ(*,70) RC
70 FORMAT(A3)
IF(RC.EQ.'ESC') GOTO 80
80 CONTINUE
READ(*,90) CHOICE
90 FORMAT (I2)

```

```

*
  IF(CHOICE.EQ.001) THEN
    I-SYSTEM('CD\\SYSTEM\\GRAPH'C)
    I-SPAWNLP(0, LOC('GRAPHER'C), LOC('GRAPHER'C),
*   LOC('TEST.GRF'C), INT4(0))
    I-SPAWNLP(0, LOC('VIEW'C), LOC('VIEW'C),
*   LOC('TEST.PLT'C), INT4(0))
    I-SYSTEM('CD\\SYSTEM\\FOR'C)
  ENDIF
  IF(CHOICE.EQ.002) THEN
    I-SYSTEM('CD\\SYSTEM\\GRAPH'C)
    I-SPAWNLP(0, LOC('GRAPHER'C), LOC('GRAPHER'C),
*   LOC('TEST.GRF'C), INT4(0))
    I-SPAWNLP(0, LOC('VIEW'C), LOC('VIEW'C),
*   LOC('TEST.PLT'C), INT4(0))
    I-SYSTEM('CD\\SYSTEM\\FOR'C)
  ENDIF
  IF(CHOICE.EQ.003) THEN
    I-SYSTEM('CD\\SYSTEM\\GRAPH'C)
    I-SPAWNLP(0, LOC('GRAPHER'C), LOC('GRAPHER'C),
*   LOC('TEST.GRF'C), INT4(0))
    I-SPAWNLP(0, LOC('VIEW'C), LOC('VIEW'C),
*   LOC('TEST.PLT'C), INT4(0))
    I-SYSTEM('CD\\SYSTEM\\FOR'C)
  ENDIF
  IF(CHOICE.EQ.004) THEN
    I-SYSTEM('CD\\SYSTEM\\GRAPH'C)
    I-SPAWNLP(0, LOC('GRAPHER'C), LOC('GRAPHER'C),
*   LOC('TEST.GRF'C), INT4(0))
    I-SPAWNLP(0, LOC('VIEW'C), LOC('VIEW'C),
*   LOC('TEST.PLT'C), INT4(0))
    I-SYSTEM('CD\\SYSTEM\\FOR'C)
  ENDIF
  IF(CHOICE.EQ.005) GOTO 1001
  GOTO 60
*
1001 CONTINUE
  RETURN
  END
*****
  SUBROUTINE SAMPLE
*****
*   This routine will take data from an existing file (RAW.TMP)   *
*   that is currently being written to from Labtech and calibrate  *
*   some of the data. The raw data as well as the calibrated data  *
*   will be written to three cumilitve files (raw data 'NAME.RAW', *
*   liquid phase data 'NAME.LIQ', and vapor phase data 'NAME.VAP'). *
*****
*
  IMPLICIT REAL*8(A-H, O-Z)
  CHARACTER*30 FILE1,FILE2,FILE3,FILE4
  CHARACTER*7 NAME
  INTEGER*2 SYSTEM
  INTEGER*2 GETDAT,GETTIM

```

```

INTEGER TYPE, YEAR, MONTH, DAY, DATE, YEARC, HOUR, MIN, SEC, HSEC, TIME, OK
*
* GET DATA SET NAME
*
WRITE(*,*)
WRITE(*,*)
WRITE(*,*) ' HERE ARE CURRENT DATA SETS ON FILE'
WRITE(*,*)
I=SYSTEM(' DIR E:\\SYSTEM\\DATA\\*.RAW' C)
5 WRITE(*,*)
WRITE(*,*) ' ENTER SYSTEM NAME EX. <CO2>'
WRITE(*,*) ' ENTER <R> TO RETURN TO MAIN MENU'
WRITE(*,*)
READ(5, '(A7)') NAME
IF(NAME.EQ.'R') GOTO 600
*
* ADD CORRECT DIRECTORY TO FILE NAME
*
* FILE1=RAW.TMP FILE3=NAME.LIQ
* FILE2=NAME.RAW FILE4=NAME.VAP
*
* FILE1='H:\RAW.TMP'
* FILE2='E:\SYSTEM\DATA\\//NAME//'.RAW'
* FILE3='E:\SYSTEM\DATA\\//NAME//'.LIQ'
* FILE4='E:\SYSTEM\DATA\\//NAME//'.VAP'
*
15 CONTINUE
OPEN(UNIT=9, ERR=16, FILE=FILE2, STATUS='OLD')
GOTO 17
16 WRITE(*,*) ' THIS DATA FILE DOES NOT EXIST AND WILL BE CREATED',
* ' IS THIS OK? (Y/N)'
READ(*, '(A1)') OK
IF(OK.EQ.'Y') THEN
OPEN(UNIT=9, FILE=FILE2, STATUS='NEW')
ENDIF
IF(OK.NE.'Y') GOTO 5
17 OPEN(UNIT=8, FILE=FILE1, SHARE='DENYNONE', STATUS='OLD')
OPEN(UNIT=10, FILE=FILE3, STATUS='UNKNOWN')
OPEN(UNIT=11, FILE=FILE4, STATUS='UNKNOWN')
*
* SET POINTER TO END OF CUMULITIVE FILES (.RAW, .LIQ, .VAP)
*
20 READ(9, *, END=21)
GOTO 20
21 BACKSPACE(9)
30 READ(10, *, END=31)
GOTO 30
31 BACKSPACE(10)
40 READ(11, *, END=41)
GOTO 40
41 BACKSPACE(11)
*
50 WRITE(6, *) 'ENTER DENSITY TYPE BEING RECORDED',
* ' (1=LIQUID, 2=VAPOR)'

```

```

READ(*,*)TYPE
IF(TYPE.EQ.1.OR.TYPE.EQ.2) GOTO 60
GOTO 50
*
60 CONTINUE
WRITE(6,*)' GATHERING RAW DATA AND CALIBRATING'
READ(8,*)
READ(8,*)TPVT,TIFT,TVDMA,TLDMA,TTAPE,PRES,PERIOD
*
* RECORD RAW DATA AND TIME STAMP
*
I=GETDAT(YEAR,MONTH,DAY)
YEARC=YEAR/100
YEARC=YEARC*100
YEAR=YEAR-YEARC
DATE=MONTH*10000+DAY*100+YEAR
I=GETTIM(HOUR,MIN,SEC,HSEC)
TIME=HOUR*100+MIN
*
WRITE(9,1000)DATE,TIME,TPVT,TIFT,TVDMA,TLDMA,TTAPE,PRES,PERIOD
WRITE(6,1001)DATE,TIME,TPVT,PRES,PERIOD
1000 FORMAT(2I12,6F12.2,F12.6)
1001 FORMAT(2I2,2F12.2,F12.6)
*
CALL DMA(TPVT,PRES,PERIOD,TYPE,DEN)
GOTO (100,200), TYPE
*
* WRITE ACQUIRED LIQUID DATA TO LIQUID FILE
*
100 CONTINUE
WRITE(10,1010)DATE,TIME,TPVT,TIFT,TVDMA,TLDMA,TTAPE,PRES,DEN
1010 FORMAT(2I12,6F12.2,F12.6)
GOTO 500
*
* WRITE ACQUIRED VAPOR DATA TO VAPOR FILE
*
200 CONTINUE
WRITE(11,1010)DATE,TIME,TTAPE,TLDMA,TVDMA,TPVT,TIFT,PRES,DEN
GOTO 500
*
500 CONTINUE
ENDFILE(8)
ENDFILE(9)
ENDFILE(10)
ENDFILE(11)
CLOSE(8)
CLOSE(9)
CLOSE(10)
CLOSE(11)
600 RETURN
END
*****
SUBROUTINE DMA(TPVT,PRES,PERIOD,TYPE,DEN)
*****

```

```

*   SUBROUTINE DMA WILL CONVERT PERIOD TO DENSITY   *
*
*   TPVT:   TEMPERATURE OF PVT CELL (F)           *
*   PRES:   SYSTEM PRESSURE (PSIA)                *
*   PERIOD:  DMA PERIOD OF SAMPLE                  *
*   TYPE:   TYPE OF DMA SAMPLE TAKEN (1-LIQUID, 2-VAPOR) *
*   DEN:    DENSITY CORRESPONDING TO DMA SAMPLE PERIOD (G/CC) *
*****
      IMPLICIT REAL*8(A-H,O-Z)
      REAL*8 K
      INTEGER TYPE
*
      TOL=10.0
*
      CALCULATE THE DENSITY OF AIR AND WATER AT SYSTEM TEMPERATURE
      AND PRESSURE
*
      IF(ABS(TPVT-120.0).LT.TOL) THEN
*
          AIR DENSITY
          A1=7.46286E-5
          B1=-1.00581E-6
*
          H2O DENSITY
          A2=0.98879
          GOTO 300
      ENDIF
*
      IF(ABS(TPVT-150.0).LT.TOL) THEN
*
          AIR DENSITY
          H2O DENSITY
          GOTO 300
      ENDIF
*
      IF(ABS(TPVT-180.0).LT.TOL) THEN
*
          AIR DENSITY
          H2O DENSITY
          GOTO 300
      ENDIF
*
      300 CONTINUE
          AIRDEN=A1*PRES +B1
          H2ODEN=A2
          GOTO (400,500) TYPE
      400 CONTINUE
*
      CALCULATE LDMA PERIOD VALUES FOR AIR AND WATER
*
      IF(ABS(TPVT-120.0).LT.TOL) THEN
          TAUAIR=3.48882 + 2.99937E-5*PRES - 2.23856E-8*PRES*PRES +
*
          1.3262E-10*PRES*PRES*PRES
          TAUH2O=3.84634 + 1.77044E-6*PRES - 1.94485E-9*PRES*PRES -
*
          1.37063E-10*PRES*PRES*PRES
          GOTO 600
      ENDIF
*

```

```
500 CONTINUE
*
*   CALCULATE VDMA PERIOD VALUES FOR AIR AND WATER
*
  IF(ABS(TPVT-120.0).LT.TOL) THEN
    TAUAIR=3.79228 + 4.72456E-5*PRES - 9.05323E-7*PRES*PRES +
*   1.3262E-10*PRES*PRES*PRES
    TAUH2O=4.04171 + 1.25814E-6*PRES + 1.54574E-8*PRES*PRES -
*   3.92157E-10*PRES*PRES*PRES
  ENDIF
*
600 CONTINUE
*
*   CALCULATE SAMPLE DENSITY
*
  K=(AIRDEN - H2ODEN)/(TAUAIR**2.0 - TAUH2O**2.0)
  DEN=K*(PERIOD**2.0-TAUH2O**2.0) + H2ODEN
  RETURN
  END
```

APPENDIX B

STEP TESTS

In order to provide Labtech Control with correct P and I constants for temperature control, step tests had to be made for the tape heater and each of the localized cartridge heaters (located near the PVT, IFT, LDMA, and VDMA cells). Figures B.1 through B.5 show the individual step tests and Figure B.6 shows a sample calculation using the method described by Smith and Corripio (30) for estimating P and I.

Basically, the method is a graphical way to estimate P and I from a step response. The following calculation is done for Figure B.6.

$$\Delta M = 5.0 \text{ Volts}$$

$$\Delta C = 4.2^\circ\text{F}$$

Where ΔM and ΔC are the manipulated variable and response variable respectively.

$$0.283(\Delta C) = 1.2^\circ\text{F}$$

$$0.632(\Delta C) = 2.7^\circ\text{F}$$

$$T_1 = 1800 \text{ sec}$$

$$T_2 = 6800 \text{ sec}$$

T_1 and T_2 are the times corresponding to 28.3% and 63.2% of the temperature increase.

$$\tau = \frac{3}{2}(T_2 - T_1) = 7500$$

$$t_0 = (0.1)\tau = 750$$

$$K = \frac{4.2}{5.0} = 0.84$$

τ is the time constant, t_0 is the dead time, and K is the gain.

With these calculated, the proportional gain may then be estimated by,

$$K_c = \frac{0.9r}{Kt_0} = 10.7$$

and the integral time as,

$$I_c = K_c/3.33t_0 = 0.0043$$

Using the above method, the individual heaters were evaluated and P and I calculated for each heater and corresponding probe. However, after initial application of these constants some of the heaters were oscillating. Therefore, some fine tuning was required. The results are presented in Table B.1

TABLE B.1
FINE-TUNED P AND I VALUES

| | |
|-------------|-----------------------|
| PVT heater | P - 3.0 I - 0.005 |
| IFT heater | P - 5.0 I - 0.005 |
| VDMA heater | P - 9.0 I - 0.005 |
| LDMA heater | P - 3.0 I - 0.005 |
| Tape heater | P - 10.0 I - 0.005 |

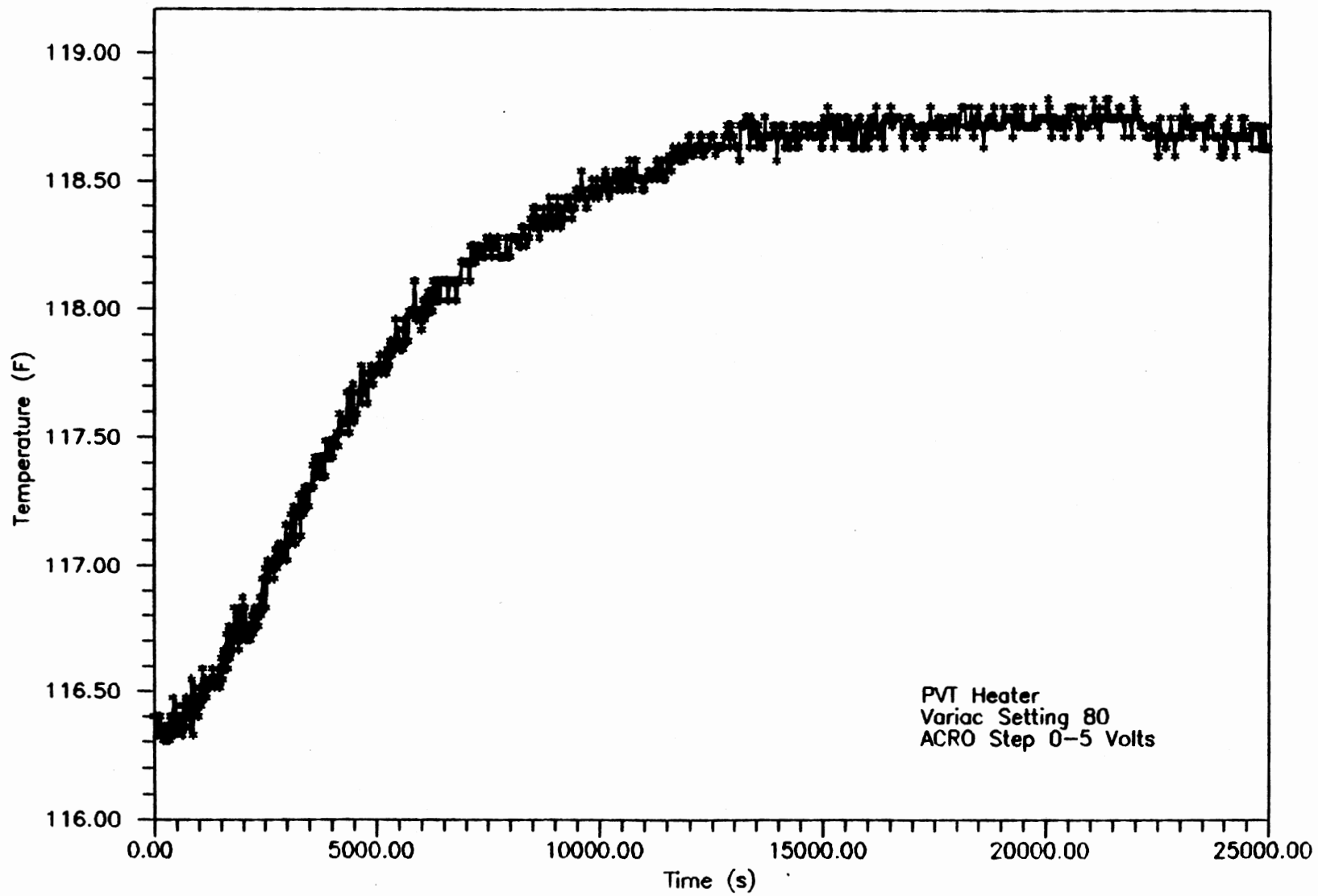


Figure B.1 PVT Heater Step Test

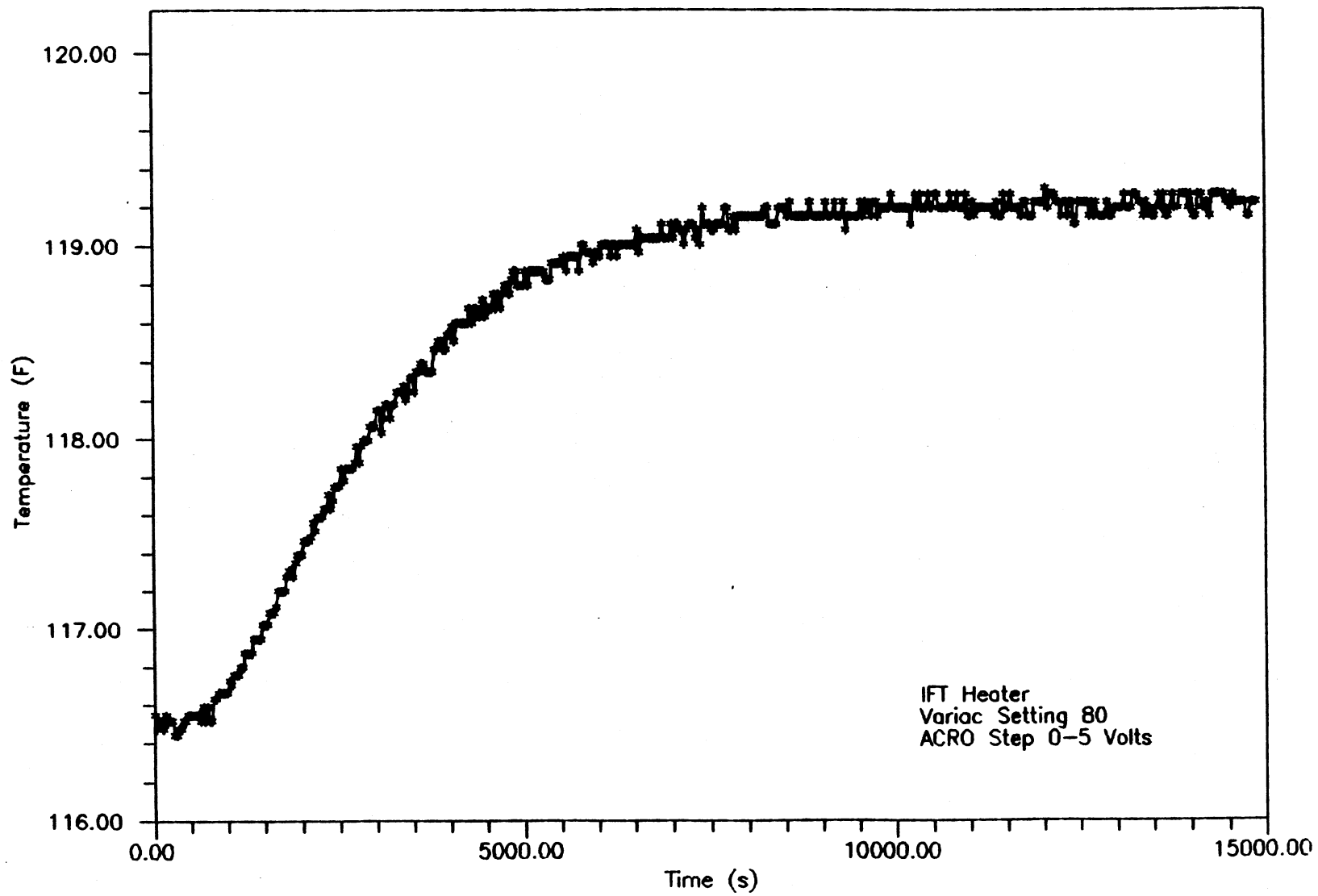


Figure B.2 IFT Heater Step Test

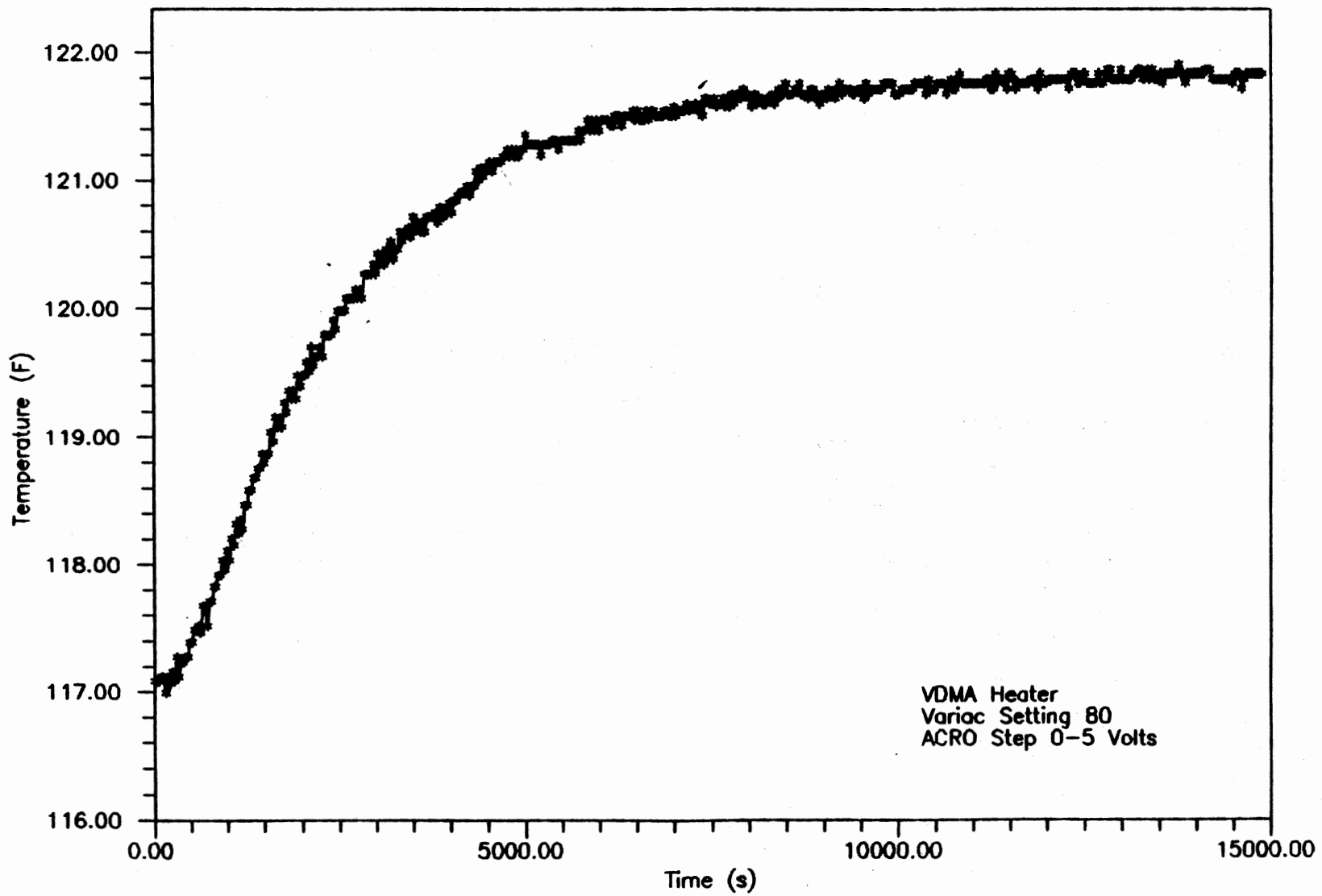


Figure B.3 VDMA Heater Step Test

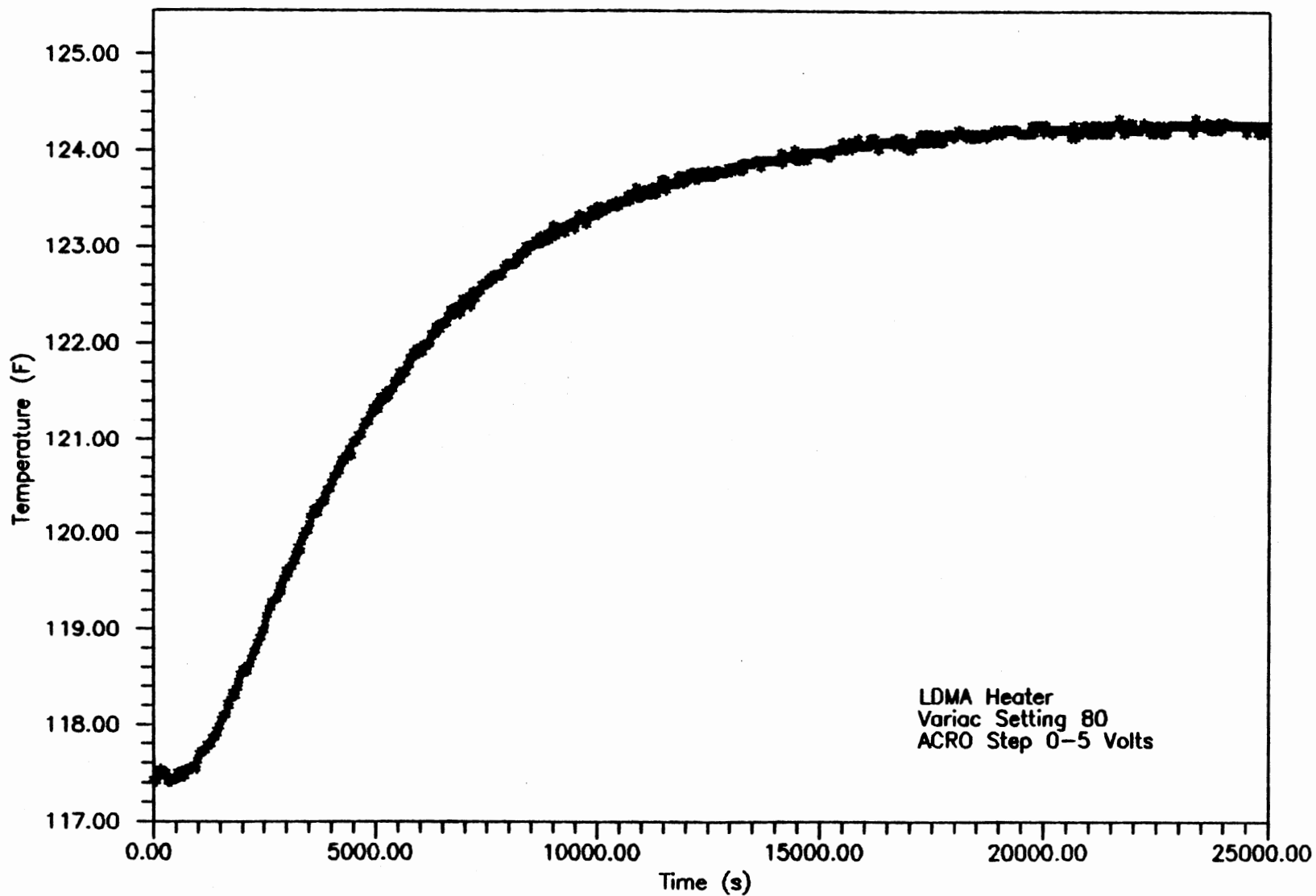


Figure B.4 LDMA Heater Step Test

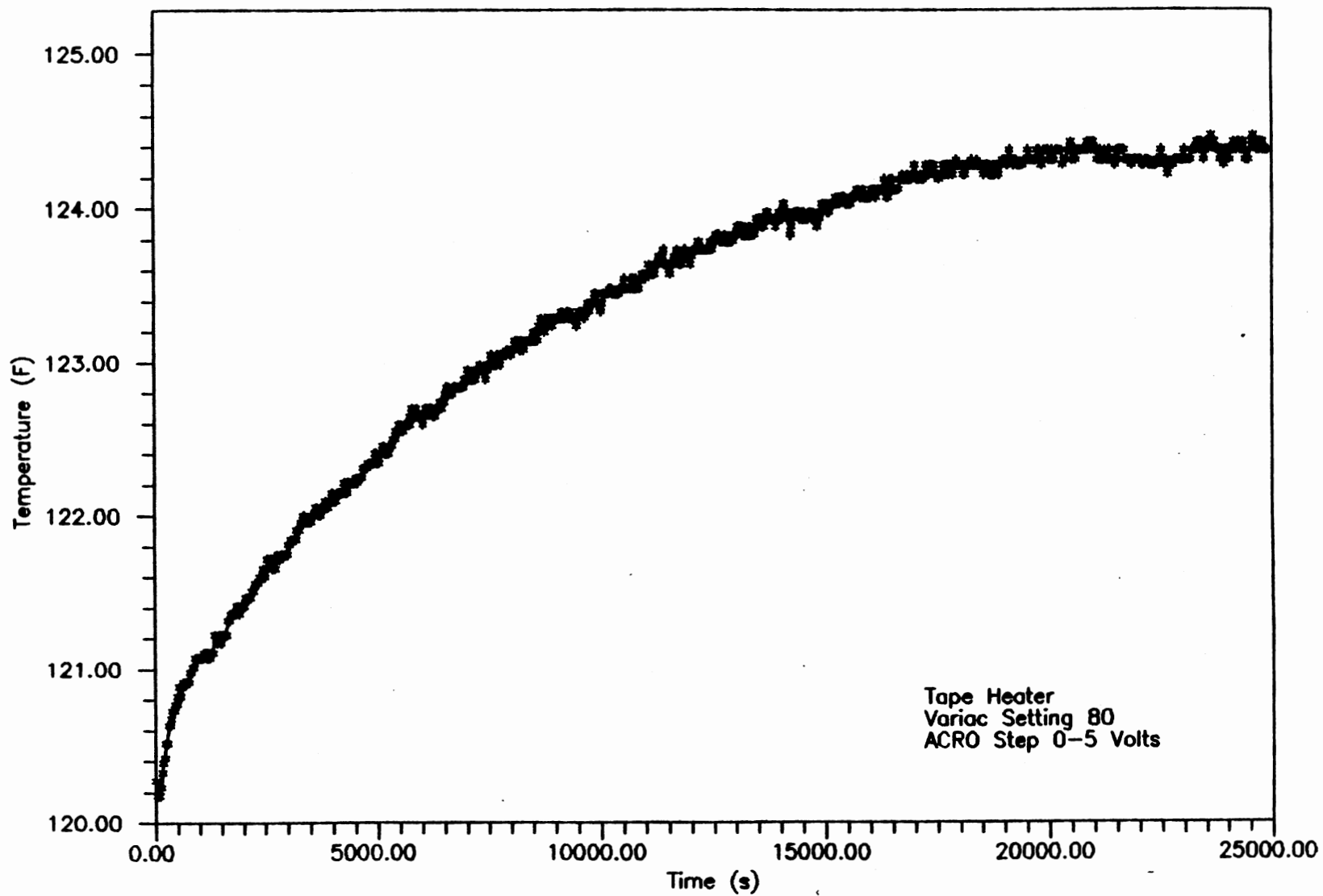


Figure B.5 Tape Heater Step Test

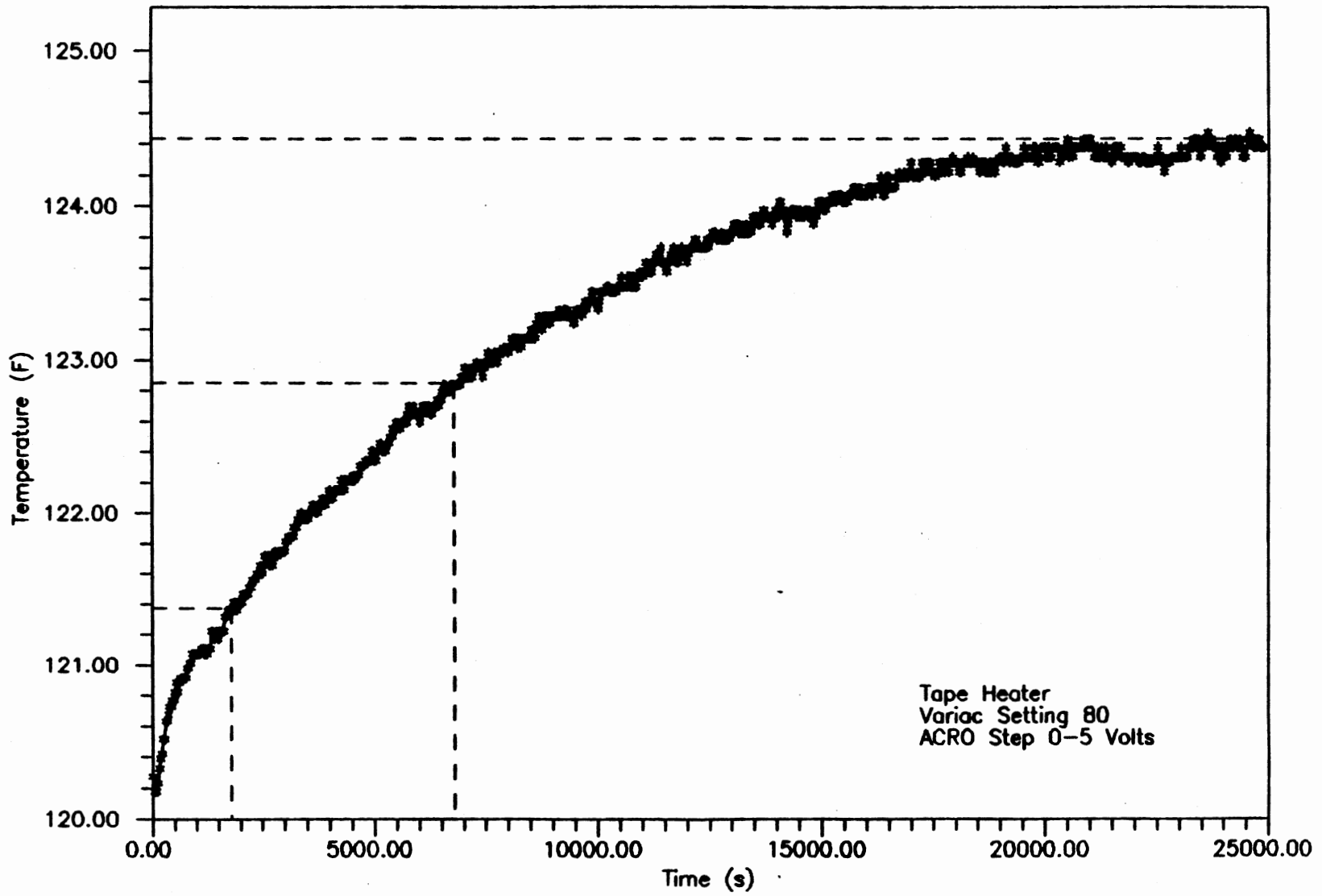


Figure B.6 Tape Heater Step Test Analysis

APPENDIX C

CALIBRATIONS

As discussed in Chapter V, the calibration of the experimental instruments is crucial to controlling the system as well as accurately measuring the properties of the fluid under study. The calibrations are performed on the thermocouples and RTD's, the pressure transducer, and the density meters.

Temperature Calibration

The temperature calibration is accomplished by positioning the thermocouples and RTD's in a common thermal environment and determining their deviations from an NBS calibrated resistance thermometer bridge. The common environment consists of an aluminum block with various size holes to hold each of the thermocouple and RTD probes as well as the probe for the resistance bridge. The system is then heated using the Watlow controller to the temperature of interest and deviations from the resistance bridge noted. Table C.1 presents the deviation of the thermocouples and RTD's at 120°F, the temperature used for the validation case.

Pressure Calibration

The pressure transducer was calibrated using a Ruska dead weight gauge utilizing weight set #23438. The gauge is designed to pull a vacuum over the weights and simultaneously float the weights with the system pressure. However, this process is very time consuming as the vacuum seal has to be broken each time the weights are varied and the vacuum re-established. An alternative approach is to pull a vacuum on a manometer and leave the opposite side open to the atmosphere. This will determine the atmospheric pressure to within 1 mm Hg which is

then added to the calculated dead weight pressure for the corrected pressure. Thus, using different weight combinations, which produce different dead weight pressures, the pressure transducer can be calibrated against the corrected dead weight pressure. Table C.2 shows the corrected dead weight calibration determined for this study.

Density Meter Calibration

As detailed in Chapter V, the period value returned by the density meter for a given sample can be converted to density by interpolation between air and water period and density values. This implies that the air and water period and density values are known at the sample temperature and pressure. Air and water densities are determined from correlations generated using reliable literature data (32,33), while the period values are obtained through calibrations over the temperature and pressure range of interest. Experience has shown that the density meter period values for a single isotherm can be represented by a simple polynomial. The polynomials are generated at each of the temperatures of interest and then incorporated into the data acquisition program for instantaneous conversion of a sample period to density. Table C.3 shows the literature density values for air at 120°F, correlation representing the data, and the deviation in the correlation. ASME (33) reports the density for water at 120°F over the 15-50 psia pressure range as constant and equal to 0.98879 g/cc. Tables C.4 and C.5 show the actual and correlated period values for air and water at 120°F over a 15-50 psia pressure range. Table C.6 shows the prediction and deviation of air densities using the polynomials for period and density, and Table C.7 shows the deviation in the prediction

of CO₂ using the air and water polynomials as a test case.

Imaging System Calibration

The imaging system requires calibration only in respect to the aspect ratio when the default PC Vision hardware calibration is used. That is, if the STARTUP.CAL file is deleted within the JAVA directory, a default calibration is generated which returns pixel values when objects are edge traced as is used in this study. However, depending on the camera and lenses used, some distortion of the true image is seen. This is alleviated by determining the Y/X ratio, or aspect ratio, and setting the appropriate parameter equal to the aspect ratio within JAVA. This is accomplished by setting FGAR = 0.77 (the aspect ratio found for this camera/lense configuration) in the AUTOEXEC.BAT file in the root directory.

Table C.1

PROBE TEMPERATURE CALIBRATIONS AT 120°F

| Probe | T (F) | Deviation (F) (Bridge - probe) |
|-----------|-------|-----------------------------------|
| Bridge | 120.1 | 0.0 |
| PVT RTD1 | 120.7 | -0.6 |
| IFT RTD2 | 121.3 | -1.2 |
| VDMA RTD3 | 121.1 | -1.0 |
| LDMA RTD4 | 121.6 | -1.5 |
| TAPE RTD5 | 120.0 | +0.1 |
| PVT TC1 | 118.2 | +1.9 |
| IFT TC2 | 118.1 | +2.0 |
| VDMA TC3 | 118.3 | +1.8 |
| LDMA TC4 | 118.6 | +1.5 |
| TAPE TC5 | 118.1 | +2.0 |

Table C.2

PRESSURE TRANSDUCER DEAD WEIGHT CALIBRATION

| Weights | Dead Wt. (psia) | Sensotec (psia) | Atmosphere (mm Hg) | Corrected Dead Wt. (psia) | Deviation (psia) D.W. - Sensotec |
|-----------|--------------------|--------------------|-----------------------|---------------------------------|-------------------------------------|
| PISTON | 2.031 | 16.20 | 743 | 16.40 | 0.20 |
| P,11 | 4.932 | 19.09 | 743 | 19.30 | 0.21 |
| P,10 | 7.832 | 21.99 | 743 | 22.20 | 0.21 |
| P,8 | 16.535 | 30.67 | 743 | 30.91 | 0.24 |
| P,8,9 | 22.336 | 36.47 | 743 | 36.71 | 0.24 |
| P,7 | 31.039 | 45.16 | 743 | 45.41 | 0.25 |
| P,7,11,12 | 35.390 | 49.51 | 743 | 49.76 | 0.25 |

Pressure calibration:

$$P (\text{correct}) = 1.00155 * P (\text{sensotec}) + 0.18$$

Table C.3

COMPARISON OF LITERATURE AND CORRELATED
DENSITY VALUES FOR AIR AT 120°F

| P (psia) | Exptl. Density (g/cc) | Calc.* Density (g/cc) | Difference Calc. - Exptl. |
|----------|--------------------------|--------------------------|------------------------------|
| 18.13 | 0.001352 | 0.001352 | 0.000000 |
| 21.76 | 0.001623 | 0.001623 | 0.000000 |
| 25.38 | 0.001893 | 0.001893 | 0.000000 |
| 29.01 | 0.002164 | 0.002164 | 0.000000 |
| 43.51 | 0.003246 | 0.003246 | 0.000000 |
| 58.02 | 0.004329 | 0.004329 | 0.000000 |

* The correlation used is given below.

$$\rho = 7.46286E-5 * P - 1.00581E-6$$

Table C.4
 ACTUAL AND CORRELATED* PERIODS FOR AIR AT 120°F

| P (psia) | PERIOD | | DIFFERENCE | | % ERROR |
|-----------------------|----------|----------|----------------|---------|---------|
| | Calc. | Exptl. | Calc. - Exptl. | | |
| ----- VDMA CELL ----- | | | | | |
| 50.05 | 3.793555 | 3.793556 | -0.000001 | -0.0000 | |
| 44.93 | 3.793428 | 3.793441 | -0.000013 | -0.0003 | |
| 40.18 | 3.793325 | 3.793328 | -0.000003 | -0.0001 | |
| 35.17 | 3.793231 | 3.793219 | 0.000012 | 0.0003 | |
| 30.03 | 3.793137 | 3.793160 | -0.000023 | -0.0006 | |
| 25.17 | 3.793046 | 3.793041 | 0.000005 | 0.0001 | |
| 20.18 | 3.792942 | 3.792947 | -0.000005 | -0.0001 | |
| 15.17 | 3.792821 | 3.792825 | -0.000004 | -0.0001 | |
| ----- LDMA CELL ----- | | | | | |
| 50.05 | 3.490282 | 3.490284 | -0.000002 | -0.0001 | |
| 44.93 | 3.490134 | 3.490137 | -0.000003 | -0.0001 | |
| 40.18 | 3.489998 | 3.490002 | -0.000004 | -0.0001 | |
| 35.17 | 3.489853 | 3.489857 | -0.000005 | -0.0001 | |
| 30.03 | 3.489704 | 3.489694 | 0.000010 | 0.0003 | |
| 25.17 | 3.489563 | 3.489583 | -0.000020 | -0.0006 | |
| 20.18 | 3.489417 | 3.489410 | 0.000007 | 0.0002 | |
| 15.17 | 3.489270 | 3.489275 | -0.000005 | -0.0001 | |

* Period correlations used are given below:

$$\text{VDMA} = 3.79228 + 4.72456\text{E-}5 * P - 9.05323\text{E-}7 * P^2 + 9.4006\text{E-}10 * P^3$$

$$\text{LDMA} = 3.48882 + 2.99937\text{E-}5 * P - 2.23856\text{E-}8 * P^2 + 1.3262\text{E-}10 * P^3$$

Table C.5

ACTUAL AND CORRELATED* PERIODS FOR WATER AT 120°F

| P (psia) | PERIOD | | DIFFERENCE | |
|-----------------------|----------|----------|----------------|---------|
| | Calc. | Exptl. | Calc. - Exptl. | % ERROR |
| ----- VDMA CELL ----- | | | | |
| 48.00 | 4.041761 | 4.041761 | 0.000000 | 0.0000 |
| 39.47 | 4.041758 | 4.041758 | 0.000000 | 0.0000 |
| 33.91 | 4.041753 | 4.041753 | 0.000000 | 0.0000 |
| 26.40 | 4.041745 | 4.041746 | -0.000001 | 0.0000 |
| 20.45 | 4.041737 | 4.041736 | 0.000001 | 0.0000 |
| 15.85 | 4.041730 | 4.041731 | -0.000001 | 0.0000 |
| ----- LDMA CELL ----- | | | | |
| 45.52 | 3.846402 | 3.846401 | 0.000001 | 0.0000 |
| 38.33 | 3.846395 | 3.846395 | 0.000000 | 0.0000 |
| 31.39 | 3.846387 | 3.846387 | 0.000000 | 0.0000 |
| 24.79 | 3.846379 | 3.846377 | 0.000002 | 0.0001 |
| 20.48 | 3.846372 | 3.846373 | -0.000001 | 0.0000 |
| 15.84 | 3.846365 | 3.846364 | 0.000001 | 0.0000 |

* Period correlations used are given below:

$$\text{VDMA} = 4.041708 + 1.25814\text{E-}6 * P + 1.54574\text{E-}8 * P^2 - 3.9216\text{E-}10 * P^3$$

$$\text{LDMA} = 3.846338 + 1.77044\text{E-}6 * P - 1.94485\text{E-}9 * P^2 - 1.3706\text{E-}10 * P^3$$

Table C.6

COMPARISON OF EXPERIMENTAL AND CALCULATED*
DENSITIES USING AIR AT 120°F

| P (psia) | DENSITY (g/cc) | | DIFFERENCE (g/cc) | %ERROR |
|-----------------------|----------------|---------|----------------------|--------|
| | Calc. | Exptl. | | |
| ----- VDMA CELL ----- | | | | |
| 50.05 | .003737 | .003734 | .000002 | 0.05 |
| 44.93 | .003403 | .003352 | .000051 | 1.52 |
| 40.18 | .003003 | .002998 | .000006 | 0.20 |
| 35.17 | .002579 | .002624 | -.000045 | -1.71 |
| 30.03 | .002329 | .002240 | .000089 | 3.97 |
| 25.17 | .001860 | .001877 | -.000017 | -0.91 |
| 20.18 | .001524 | .001505 | .000019 | 1.26 |
| 15.17 | .001146 | .001131 | .000015 | 1.33 |
| ----- LDMA CELL ----- | | | | |
| 50.05 | .003740 | .003734 | .000006 | 0.16 |
| 44.93 | .003359 | .003352 | .000007 | 0.21 |
| 40.18 | .003009 | .002998 | .000011 | 0.37 |
| 35.17 | .002634 | .002624 | .000010 | 0.38 |
| 30.03 | .002213 | .002240 | -.000027 | -1.21 |
| 25.17 | .001930 | .001877 | .000053 | 2.82 |
| 20.18 | .001486 | .001505 | -.000019 | -1.26 |
| 15.17 | .001143 | .001131 | .000012 | 1.06 |

* Calculated using interpolation formula discussed in chapter V and correlations from tables C.3 -C.5.

Table C.7

COMPARISON OF EXPERIMENTAL* AND CALCULATED**
DENSITIES USING CO₂ AT 120°F

| P (psia) | DENSITY (g/cc) | | DIFFERENCE (g/cc) | %ERROR |
|-----------------------|----------------|----------|----------------------|--------|
| | Calc. | Exptl. | | |
| ----- VDMA CELL ----- | | | | |
| 49.13 | 0.005588 | 0.005638 | -0.000050 | -0.89 |
| 45.18 | 0.005121 | 0.005179 | -0.000058 | -1.12 |
| 40.20 | 0.004479 | 0.004602 | -0.000123 | -2.67 |
| 35.19 | 0.003866 | 0.004023 | -0.000157 | -3.90 |
| 30.17 | 0.003252 | 0.003444 | -0.000192 | -5.57 |
| 25.23 | 0.002640 | 0.002876 | -0.000236 | -8.21 |
| 20.20 | 0.002054 | 0.002299 | -0.000245 | -10.66 |
| 15.22 | 0.001552 | 0.001730 | -0.000178 | -10.29 |
| ----- LDMA CELL ----- | | | | |
| 49.18 | 0.005683 | 0.005644 | 0.000039 | 0.69 |
| 45.21 | 0.005293 | 0.005183 | 0.000110 | 2.12 |
| 40.21 | 0.004685 | 0.004603 | 0.000082 | 1.78 |
| 35.20 | 0.004171 | 0.004024 | 0.000147 | 3.65 |
| 30.17 | 0.003603 | 0.003444 | 0.000159 | 4.62 |
| 25.23 | 0.003027 | 0.002876 | 0.000151 | 5.25 |
| 20.20 | 0.002430 | 0.002299 | 0.000131 | 5.70 |
| 15.22 | 0.001827 | 0.001730 | 0.000097 | 5.61 |

* Experimental values from IUPAC

** Calculated using interpolation formula discussed in
chapter V and correlations from tables C.3 - C.5.

APPENDIX D

ERROR ANALYSIS

In any research environment there exist two types of errors when measuring experimental values: random and systematic errors. Random non-recurring errors can be treated statistically. Systematic errors, however, are eliminated by repeated calibration of the experimental instruments and careful external checks against reliable data. In this study, the experimental equipment was calibrated before the data acquisition run and in some instances, specifically temperature, the calibration was done at intermediate steps along the study. The pressure transducer was calibrated with a dead weight gauge and by comparing the vapor pressure of the pure fluid being studied with literature values. The density meters were calibrated with air and water and a CO₂ run was done to test the reliability of the calibration before the initial study was started.

Evaluation of random errors begins with estimating the errors of each recorded value and determining how these errors propagate through calculations using the recorded values. Following numerous calibrations, specifically with NBS certified thermometers, dead weight gauges, and pure fluids, the errors associated with each measurable quantity was estimated as follows:

$$\epsilon_T = 0.1^\circ\text{F}$$

$$\epsilon_P = 0.05 \text{ psia}$$

$$\epsilon_D = 0.00005$$

where ϵ_T , ϵ_P , and ϵ_D are the errors associated with temperature, pressure, and the density meter period, respectively. The error in the determination of density, must be determined by analysis of how the above errors propagate in the calculation of density. The error

propagation is determined in the following manner.

$$\rho = f(\tau, \tau_a, \tau_w, \rho_a, \rho_w)$$

$$\rho = \frac{(\rho_a - \rho_w)}{(\tau_a^2 - \tau_w^2)} \cdot (\tau_w^2 - \tau^2) + \rho$$

$$\sigma_\rho^2 = \left(\frac{\partial \rho}{\partial \tau} \right)^2 \sigma_\tau^2 + \left(\frac{\partial \rho}{\partial \tau_a} \right)^2 \sigma_{\tau_a}^2 + \left(\frac{\partial \rho}{\partial \tau_w} \right)^2 \sigma_{\tau_w}^2 + \left(\frac{\partial \rho}{\partial \rho_a} \right)^2 \sigma_{\rho_a}^2 + \left(\frac{\partial \rho}{\partial \rho_w} \right)^2 \sigma_{\rho_w}^2$$

$$\left(\frac{\partial \rho}{\partial \tau} \right) = \frac{2(\rho_a - \rho_w)}{(\tau_a^2 - \tau_w^2)} \tau$$

$$\left(\frac{\partial \rho}{\partial \tau_a} \right) = - \frac{2(\rho_a - \rho_w)(\tau^2 - \tau_w^2)\tau_a}{(\tau_a^2 - \tau_w^2)^2}$$

$$\left(\frac{\partial \rho}{\partial \tau_w} \right) = \frac{-2(\tau_a^2 - \tau_w^2)(\rho_a - \rho_w)\tau_w + 2(\tau^2 - \tau_w^2)(\rho_a - \rho_w)\tau_w}{(\tau_a^2 - \tau_w^2)^2}$$

$$\left(\frac{\partial \rho}{\partial \rho_a} \right) = \frac{(\tau^2 - \tau_w^2)}{(\tau_a^2 - \tau_w^2)}$$

$$\left(\frac{\partial \rho}{\partial \rho_w} \right) = \frac{-(\tau^2 - \tau_w^2)}{(\tau_a^2 - \tau_w^2)} + 1$$

Now calculating the errors,

$$\sigma_\tau = \epsilon_\tau = 0.00005$$

$$\sigma_{\tau_a}^2 = \epsilon_\tau^2 + \left(\frac{\partial \tau_a}{\partial \tau} \right)^2 \sigma_\tau^2 + \left(\frac{\partial \tau_a}{\partial \rho} \right)^2 \sigma_\rho^2$$

Although not presented here, a simple mapping of the period dependence on temperature and pressure for air and water was done. This allowed for the prediction of error for density accounting for temperature and pressure. The results described below were done using the VDMA cell.

$$\tau_w = [(-0.067804 * T(K) + 32.7759) * 1E-7] * P(\text{psia}) \\ + 0.000747 * T(K) + 3.80146$$

$$\left(\frac{\partial \tau_a}{\partial T} \right) = (-0.006807 * P * 1E-5) + 0.000822$$

$$\left(\frac{\partial \tau_a}{\partial P} \right) = (-0.006807 * T + 4.21754) * 1E-5$$

$$\sigma_T = \epsilon_T = 0.1^\circ \text{F}$$

$$\sigma_P = \epsilon_P = 0.05 \text{ psia}$$

$$\sigma_{\tau_a}^2 = 0.00005^2 + [-0.006807 * P * 1E-5 + 0.000822]^2 * 0.0056 \\ + [(-0.006807 * T + 4.21754) * 1E-5]^2 * 0.0025$$

Similarly with τ_w

$$\sigma_{\tau_w}^2 = 0.00005^2 + [-0.067804 * P * 1E-7 + 0.000747]^2 * 0.0056 \\ + [(-0.067804 * T + 32.7759) * 1E-7]^2 * 0.0025$$

$$\sigma_{\rho_a} = \epsilon_{\rho_a} = 0.001 \text{ g/cc}$$

$$\sigma_{\rho_w} = \epsilon_{\rho_w} = 0.001 \text{ g/cc}$$

Therefore, substituting typical values:

$$\begin{aligned} T &= 150^\circ \text{F} = 339 \text{ K} \\ P &= 25.0 \text{ psia} \\ \tau_a &= 3.806500 \\ \tau_w &= 4.054500 \\ \tau &= 3.954000 \\ \rho_a &= 0.0018 \text{ g/cc} \\ \rho_w &= 0.98 \text{ g/cc} \end{aligned}$$

gives a typical error for σ_ρ as 0.0008 g/cc, or 0.001 g/cc.

The IFT reproducibility for the various needles employed in this study can be estimated from Table II. Clearly, the largest needle diameter (0.0355 inch) produces an IFT value with the least amount of variation. Thus, the 0.0355 inch needle diameter is likely to be the optimum tip diameter for the IFT measurement, and consequently the resultant IFT value is best.

The expected uncertainty for this most stable estimate of the IFT is about 0.5%. The estimate for the uncertainty, however, does not include the variations due to errors in the phase density difference. Following is an error propagation which accounts for these variations in the IFT measurement:

$$\gamma = \left(\frac{\gamma}{\Delta\rho} \right) \Delta\rho = \text{IFTR}\Delta\rho$$

$$\sigma_\gamma^2 = \left(\frac{\partial\gamma}{\partial\text{IFTR}} \right)^2 \sigma_{\text{IFTR}}^2 + \left(\frac{\partial\gamma}{\partial\Delta\rho} \right)^2 \sigma_{\Delta\rho}^2$$

$$\sigma_\gamma^2 = \Delta\rho \sigma_{\text{IFTR}}^2 + \sigma_{\Delta\rho}^2$$

$$\sigma_{\text{IFTR}}^2 = [(0.005)\text{IFTR}]^2$$

$$\sigma_{\Delta\rho}^2 = 2\sigma_{\rho}^2 = 2(0.001)^2 = 2.0\text{E-}6 \text{ g}^2/\text{cm}^6$$

Substituting typical values for R and $\Delta\rho$,

$$\text{IFTR} = 21.2$$

$$\Delta\rho = 0.5917 \text{ g/cc}$$

yields $\sigma_{\gamma} = 0.08 \text{ dyne-cm}$ or 0.6%

Repeating the above analysis using the σ_{IFTR} obtained from the complete data set results in $\sigma_{\gamma} = 0.37 \text{ dyne-cm}$ or 3%.

The following is a typical output from the numerical integration routine provided by Pallas.

n-Pentane 120.0 F, 6/5/91

| | |
|---|---|
| PRINT RESIDUAL SUMMARY EACH ITERATION | 0 |
| PRINT EIGENVECTORS & EIGENVALUES EACH ITERATION | 0 |
| PRINT PARAMETER ESTIMATION SUMMARY EACH ITERATION | 0 |
| PRINT DATA TABLES | 1 |
| PRINT RESULT SUMMARY FOR EACH DATA SET | 1 |

| | |
|--------------------------------|------|
| UNIT NUMBER FOR DATA SET INPUT | 10 |
| DROP TYPE | 1 |
| NUMBER OF POINTS TO CALCULATE | 3000 |
| NUMBER OF POINTS TO OUTPUT | 100 |
| MAXIMUM NUMBER OF ITERATIONS | 40 |

| | |
|-----------------------------------|-----------|
| DENSITY DIFFERENCE (GM/CC) | .5917E+00 |
| Z COORDINATE OF TIP (Z PIXEL) | .0000E+00 |
| MAGNIFICATION FACTOR (X PIXEL/CM) | .1000E+01 |
| SIGNIFICANCE LEVEL | .9500E+00 |

INITIAL PARAMETER ESTIMATES

| | |
|--|-----------|
| TILT ANGLE (THETA - DEGREES) | .0000E+00 |
| ASPECT RATIO (ASPECT - Z PIXEL/X PIXEL) | .1000E+01 |
| X COORDINATE OF THE APEX (XAPEX - X PIXEL) | .0000E+00 |
| Z COORDINATE OF THE APEX (ZAPEX - Z PIXEL) | .0000E+00 |
| RADIUS OF CURVATURE AT THE APEX (RADIUS - Z PIXEL) | .0000E+00 |
| INTERFACIAL TENSION (GAMMA - DYNES/CM) | .1260E+02 |

SCALE FACTORS FOR THE PARAMETERS

| | |
|--|-----------|
| THETA (DEGREES) | .1000E+01 |
| ASPECT (FRACTION) | .5000E-01 |
| XAPEX (FRACTION OF DROP WIDTH) | .5000E-01 |
| ZAPEX (FRACTION OF DROP WIDTH) | .5000E-01 |
| RADIUS (FRACTION OF DROP WIDTH) | .2000E+00 |
| GAMMA (MULTIPLIER OF INITIAL ESTIMATE) | .1500E+01 |

FIXED (0) OR FREE (1) PARAMETERS

| | |
|--------|---|
| THETA | 0 |
| ASPECT | 0 |
| XAPEX | 1 |
| ZAPEX | 1 |
| RADIUS | 1 |

GAMMA 1

CONVERGENCE CRITERIA

| | |
|---|-----------|
| ABSOLUTE PARAMETER CHANGE | .1000E-07 |
| RELATIVE PARAMETER CHANGE | .1000E-07 |
| RELATIVE CHANGE IN THE OBJECTIVE FUNCTION | .1000E-15 |
| DERIVATIVE OF THE OBJECTIVE FUNCTION | .1000E-15 |
| MAXIMUM PERMITTED JUMP LENGTH | .2000E+00 |

DATA SET 1
TIME 0 SEC

DROP SHAPE DATA

| X PIXEL | Z PIXEL |
|-------------|-------------|
| -.62210E-01 | .00000E+00 |
| -.62997E-01 | -.30750E-02 |
| -.64569E-01 | -.61500E-02 |
| -.66142E-01 | -.92240E-02 |
| -.67715E-01 | -.12271E-01 |
| -.69287E-01 | -.15345E-01 |
| etc... | |

INITIAL PARAMETER ESTIMATES

| | |
|--------|--------------------|
| THETA | .0000D+00 DEGREES |
| ASPECT | .1000D+01 FRACTION |
| XAPEX | .7975D-03 CM |
| ZAPEX | -.2095D+00 CM |
| RADIUS | .1097D+00 CM |
| GAMMA | .1260D+02 DYNES/CM |

CONVERGENCE WAS OBTAINED DUE TO ACCEPTABLE
ABSOLUTE CHANGE IN THE TRANSFORMED PARAMETERS

| | |
|---------------------------------|-------------|
| ITERATIONS | 6 |
| NUMBER OF FREE PARAMETERS | 4 |
| OBJECTIVE FUNCTION | .264248D-04 |
| AVERAGE OF RESIDUALS | .192623D-06 |
| ROOT MEAN SQUARE OF RESIDUALS | .398980D-03 |
| STANDARD DEVIATION OF RESIDUALS | .403876D-03 |

FINAL PARAMETER ESTIMATES WITH "INNER" AND "OUTER" CONFIDENCE LIMITS

| XAPEX CM | ZAPEX CM | RADIUS CM | GAMMA DYNES/CM |
|-------------|--------------|--------------|-------------------|
| .985750D-03 | -.209303D+00 | .871157D-01 | .125429D+02 |
| .985750D-03 | -.209303D+00 | .871157D-01 | .125429D+02 |
| .985750D-03 | -.209303D+00 | .871157D-01 | .125429D+02 |
| .985750D-03 | -.209303D+00 | .871157D-01 | .125429D+02 |
| .985750D-03 | -.209303D+00 | .871157D-01 | .125429D+02 |

| | |
|------------------------------|-------------|
| NUMBER OF CALCULATED POINTS | 3773 |
| NUMBER OF POINTS OUTPUT | 103 |
| NUMBER OF DATA POINTS | 166 |
| MINIMUM NUMBER OF SEARCHES | 0 |
| MAXIMUM NUMBER OF SEARCHES | 110 |
| AVERAGE NUMBER OF SEARCHES | .140293D+02 |
| MAXIMUM CALCULATED Z | |
| (FROM APEX) | .209303D+00 |
| (FROM ORIGIN) | .183366D-16 |
| ARC LENGTH INCREMENT (CM) | .141393D-03 |
| SURFACE AREA OF DROP (CM**2) | .116517D+00 |
| VOLUME OF DROP (CM**3) | .418880D-02 |
| CONTACT ANGLE (DEGREES) | .114643D+03 |

| X (TRANS) (CM) | Z (TRANS) (CM) | X (CALC) (CM) | Z (CALC) (CM) | RESIDUAL (CM) |
|-------------------|-------------------|------------------|------------------|------------------|
| -.631958D-01 | .209303D+00 | -.622923D-01 | .208888D+00 | -.994193D-03 |
| -.639828D-01 | .206228D+00 | -.636018D-01 | .206051D+00 | -.419852D-03 |
| -.655548D-01 | .203153D+00 | -.650573D-01 | .202921D+00 | -.548810D-03 |
| -.671278D-01 | .200079D+00 | -.665163D-01 | .199793D+00 | -.674716D-03 |
| -.687008D-01 | .197032D+00 | -.679636D-01 | .196689D+00 | -.813031D-03 |
| etc.. | | | | |

SUMMARY FOR ALL DATA SETS

| | |
|--------------------------------|-------------|
| NUMBER OF DATA SETS | 1 |
| NUMBER OF CONVERGENCE FAILURES | 0 |
| CONVERGENCES BY EPSP | 1 |
| CONVERGENCES BY EPSR | 0 |
| CONVERGENCES BY EPSQ | 0 |
| CONVERGENCES BY EPSD | 0 |
| NUMBER OF CUT BACKS | 0 |
| AVERAGE ITERATIONS | .600000D+01 |
| OBJECTIVE FUNCTION | .264248D-04 |
| AVERAGE OF RESIDUALS | .192623D-06 |

| | |
|---------------------------------|-------------|
| ROOT MEAN SQUARE OF RESIDUALS | .398980D-03 |
| STANDARD DEVIATION OF RESIDUALS | .403876D-03 |
| AVERAGE DROP AREA (CM**2) | .116517D+00 |
| AVERAGE DROP VOLUME (CM**3) | .418880D-02 |
| AVERAGE CONTACT ANGLE (DEGREES) | .114643D+03 |

AVERAGE PARAMETER ESTIMATES WITH "INNER" AND "OUTER" CONFIDENCE LIMITS

| XAPEX CM | ZAPEX CM | RADIUS CM | GAMMA DYNES/CM |
|-------------|--------------|--------------|-------------------|
| .985750D-03 | -.209303D+00 | .871157D-01 | .125429D+02 |
| .985750D-03 | -.209303D+00 | .871157D-01 | .125429D+02 |
| .985750D-03 | -.209303D+00 | .871157D-01 | .125429D+02 |
| .985750D-03 | -.209303D+00 | .871157D-01 | .125429D+02 |
| .985750D-03 | -.209303D+00 | .871157D-01 | .125429D+02 |

2

VITA

Kurtis V. Roush

Candidate for the Degree of

Master of Science

Thesis: AUTOMATED PHASE DENSITIES AND INTERFACIAL TENSION MEASUREMENTS

Major Field: Chemical Engineering

Biographical:

Personal Data: Born in Santa Barbara, California, October 27, 1966, the son of Jerry and Kay Roush. Married to Lori Wick on August 12, 1989.

Education: Graduated from Broken Arrow High School, Broken Arrow, Oklahoma, in May 1984; received Bachelor of Science Degree in Chemical Engineering from Oklahoma State University in December, 1989; completed requirements for Master of Science Degree at Oklahoma State University in July, 1991.

Professional Experience: Employed by Warren Petroleum as summer engineer, Summer, 1988; Employed by British Petroleum as a summer engineer, summer 1989 and 1990; Research Assistant, School of Chemical Engineering, Oklahoma State University, May, 1987 to July, 1991.
Member of American Institute of Chemical Engineers and Omega Chi Epsilon